HHS Public Access

Author manuscript

Neurobiol Dis. Author manuscript; available in PMC 2021 September 07.

Published in final edited form as:

Neurobiol Dis. 2021 July ; 155: 105393. doi:10.1016/j.nbd.2021.105393.

Early Decreases in Cortical Mid-Gamma Peaks Coincide with the Onset of Motor Deficits and Precede Exaggerated Beta Build-up in Rat Models for Parkinson's Disease

Elena Brazhnik[a,*], **Nikolay Novikov**[a,*], **Alex J. McCoy**[a], **Neda M. Ilieva**[a], **Marian W. Ghraib**[a], **Judith R. Walters**[a,†]

[a]Neurophysiological Pharmacology Section, National Institute of Neurological Disorders and Stroke, National Institutes of Health, Bethesda, MD 20892-3702

Abstract

Evidence suggests that exaggerated beta range local field potentials (LFP) in basal ganglia-thalamocortical circuits constitute an important biomarker for feedback for deep brain stimulation in Parkinson's disease patients, although the role of this phenomenon in triggering parkinsonian motor symptoms remains unclear. A useful model for probing the causal role of motor circuit LFP synchronization in motor dysfunction is the unilateral dopamine cell-lesioned rat, which shows dramatic motor deficits walking contralaterally to the lesion but can walk steadily ipsilaterally on a circular treadmill. Within hours after 6-OHDA injection, rats show marked deficits in ipsilateral walking with early loss of significant motor cortex (MCx) LFP peaks in the mid-gamma 41–45 Hz range in the lesioned hemisphere; both effects were reversed by dopamine agonist administration. Increases in MCx and substantia nigra pars reticulata (SNpr) coherence and LFP power in the 29–40 Hz range emerged more gradually over 7 days, although without further progression of walking deficits. Twice-daily chronic dopamine antagonist treatment induced rapid onset of catalepsy and also reduced MCx 41–45 Hz LFP activity at 1 h, with increases in MCx and SNpr 29–40 Hz power/coherence emerging over 7 days, as assessed during periods of walking before the morning treatments. Thus, increases in high beta power in these parkinsonian models emerge gradually and are not linearly correlated with motor deficits. Earlier changes in cortical circuits, reflected in the rapid decreases in MCx LFP mid-gamma LFP activity, may contribute to evolving plasticity

[†]Correspondence should be addressed to Judith R. Walters, Ph.D., Neurophysiological Pharmacology Section, NINDS, NIH, 35 Convent Drive, Building 35 Room 1C903, Bethesda, MD 20892-3702 USA waltersj@ninds.nih.gov.

[*]E.B. and N.N. contributed equally to this work and are co-first authors.

Credit author statement

Elena Brazhnik: Conceptualization, Methodology, Validation, Formal Analysis, Investigation, Data Curation, Visualization, Writing -Original Draft, Supervision, Writing – Review and Editing.

Nikolai Novikov: Conceptualization, Methodology, Formal analysis, Investigation, Writing-original draft, Writing - Review and Editing.

Alex McCoy: Software, Formal analysis, Data Curation, Visualization, Writing – Original Draft, Writing – Review and Editing

Marian Ghraib, Software, Validation, Formal analysis, Data Curation

Neda Ilieva: Formal Analysis

Judith Walters: Conceptualization, Resources, Writing-Review and Editing, Supervision, Project Administration

Declaration of Competing Interest: None

supporting increased beta range synchronized activity in basal ganglia-thalamocortical circuits after loss of dopamine receptor stimulation.

Keywords

Parkinson's disease; Movement disorders; Local field potentials; Beta oscillations; Gamma oscillations; Motor cortex; Substantia nigra pars reticulata; Basal ganglia; Gait; Dopamine antagonists; Rodent models

1. Introduction

The presence of prominent synchronized oscillatory local field potential activity and spiking in the beta range (13 – 35 Hz) in the subthalamic nucleus (STN), globus pallidus internus and motor cortex (MCx) of Parkinson's patients was first observed 2 decades ago, during implantation of deep brain stimulation (DBS) electrodes for the treatment of Parkinson's disease (PD) (Levy et al., 2000; Brown et al., 2001; Marsden et al., 2001; Cassidy et al., 2002; Williams et al., 2002). This was notable, in part, because, in healthy individuals, beta range oscillatory activity in the MCx was thought to be involved in maintenance of an idling state, with initiation of movement associated with desynchronization of the beta oscillations followed, at variable intervals, by rebound or resynchronization (Pfurtscheller et al., 1996; Sochurkova and Rektor, 2003). It seemed possible, therefore, that in PD patients, the increased synchronization of beta activity in the basal ganglia and MCx might impair or delay movement initiation, producing bradykinesia and rigidity (Levy et al., 2002; Brown, 2003; Dostrovsky et al., 2004; Hutchison et al., 2004).

In subsequent years, researchers have probed the nature of the relationship between this exaggerated beta range activity and the motor deficits associated with loss of dopamine. Studies have shown that reductions in motor symptoms associated with levodopa (L-dopa) or dopamine agonist therapy and/or DBS are significantly correlated with reductions in beta range activity in the STN (Priori et al., 2004; Kuhn et al., 2006; Giannicola et al., 2010; Whitmer et al., 2012; Quinn et al., 2015; Neumann et al., 2016; Oswal et al., 2016), further suggesting that increases in beta activity might play a causal role in the generation of bradykinesia. Moreover, movements such as tapping, reaching and walking were found to be associated with event-related desynchronization/resynchronization or amplitude modulation of the beta signal in recordings from PD patients (Kuhn et al., 2004; Heinrichs-Graham et al., 2017; Fischer et al., 2018; Hell et al., 2018). However, the causative role of the exaggerated beta activity in the generation of bradykinesia has remained a matter of debate (Kuhn et al., 2008; Quiroga-Varela et al., 2013; Stein and Bar-Gad, 2013; Brittain and Brown, 2014; Mallet et al., 2019; Swan et al., 2019; Wichmann, 2019).

As clinical studies are currently exploring the utility of using increases in beta power and, more specifically, bursts of STN beta activity, as triggers for closed-loop DBS (Hell et al., 2019; Lofredi et al., 2019; Little and Brown, 2020; Tinkhauser et al., 2020), further insight into how these signals emerge and their role in the expression of motor symptoms could prove useful in maximizing their efficacy as biomarkers.

Animal models for PD provide a means of obtaining insight into the significance of the exaggerated oscillatory activity evident in the basal ganglia-thalamocortical circuits after loss of dopamine. Rat models of PD in particular have been useful for these studies (Dejean et al., 2008; Cruz et al., 2009; Ellens and Leventhal, 2013; Stein and Bar-Gad, 2013; Nevado-Holgado et al., 2014; Javor-Duray et al., 2015). The aim of the present investigation was to use several different strategies for reducing dopamine receptor stimulation in the rat to identify the earliest changes in oscillatory LFP power and spiking activity in MCx and SNpr that consistently correlate with early changes in motor function. A further goal was to perform the neurophysiological recordings while maintaining animals in a stable behavioral state which allowed simultaneous on-going assessment of the emergence of motor deficits relevant to PD.

A behavioral state that seemed suitable is walking, which is notably impaired in PD patients (Warlop et al., 2016; Mirelman et al., 2019; Park et al., 2020) as well as in the dopamine-depleted rat. Rats with a unilateral 6-OHDA-induced dopamine cell lesion display difficulties walking in the circular treadmill in the direction contralateral to the lesion, but can make more consistent progress, in spite of impaired stepping, while walking in the direction ipsilateral to the dopamine cell lesion (Avila et al., 2010; Brazhnik et al., 2012; Delaville et al., 2014). In the present study the circular treadmill was used to assess the time frame of the early changes in LFP power and peak frequency, coherence, and correlated spiking in the high beta (29–35 Hz), high beta/low gamma (HB/LG, 29–40 Hz) and mid-gamma (40–55 Hz) ranges in conjunction with motor deficits in 3 models of PD. Three different rat models of Parkinson's disease were used: (1) unilateral and bilateral 6-hydroxydopamine (6-OHDA)-induced dopamine cell lesions; (2) chronic D1 and D2 (D1+D2) dopamine receptor antagonist treatments; or (3) acute tetrodotoxin (TTX) infusion into the median forebrain bundle (MFB). Results showed the most immediate early change emerging in conjunction with motor deficits across the three parkinsonian models was a reduction in the incidence of dominant peaks in MCx LFP power spectra in the mid-gamma (41–55) range. This preceded the more gradual increases in high beta (29–40Hz) LFP power in the MCx and SNpr.

2. Materials and Methods

All experimental procedures were conducted in accordance with the NIH Guide for Care and Use of Laboratory Animals and approved by the NINDS Animal Care and Use Committee. Every effort was made to minimize the number of animals used and their discomfort.

2.1 Animals

Male Long-Evans rats (Taconic Farm, Hudson, NY, USA), weighing 250–300 g were housed with *ad libitum* access to food and water in environmentally controlled conditions with a reversed 12:12hr light:dark cycle (lights on 6 PM to 6 AM).

Nineteen rats were implanted with electrode bundles in the MCx and SNpr, and a guide cannula in the medial forebrain bundle (MFB) for subsequent injection of the neurotoxin 6-OHDA HBr (Sigma-Aldrich) into the MFB to induce dopamine cell lesion. Sixteen of these rats were implanted unilaterally in the left hemisphere, and 3 were implanted bilaterally. Ten

of the unilaterally implanted rats (Group 1) and the three bilaterally implanted rats (Group 2) were used to investigate the emergence and evolution of oscillatory activity in the high beta/mid-gamma frequency range in the MCx-basal ganglia network in conjunction with the development of motor deficits over the first week after 6-OHDA infusion. The remaining 6 unilaterally implanted rats (Group 3) were administered a dopamine agonist, apomorphine, over the first 2 days following 6-OHDA administration to examine the effects of increasing dopamine receptor stimulation on early changes in MCx and SNpr LFP activity and motor function.

Three additional rats (Group 4) were unilaterally (2 rats) or bilaterally (1 rat) implanted with electrode bundles in the MCx and SNpr and guide cannulas in the MFB to explore the effect of tetrodotoxin (TTX)-induced acute blockade of axonal transmission in the nigrostriatal pathway (Galati et al., 2009).

Ten rats (Group 5) were used to investigate the changes in high beta/mid-gamma frequency LFP activity in a second model for reduction of dopamine receptor stimulation involving chronic blockade of D1 and D2 dopamine receptors via twice daily injections of D1+D2 dopamine antagonists over 7 days. Four of these rats were implanted unilaterally and 6 were implanted bilaterally with MCx and SNpr electrode bundles (16 hemispheres total).

The final group of 5 rats (Group 6) was implanted bilaterally with electrode bundles in the MCx and SNpr and also received unilateral injections of 6-OHDA into the MFB (left hemisphere) during the same surgery. After one week of recovery, these rats were treated twice daily with D1+D2 antagonists over 7 days to compare changes in LFP in the MCx and SNpr in the DA-cell lesioned hemisphere with those in the non-lesioned hemisphere during periods of catalepsy induced by the dopamine antagonist treatments.

2.2. Behavioral training

A week before surgeries, rats were handled daily and trained to walk on a continuously rotating circular treadmill (Avila et al., 2010). Training consisted of 3–5 daily sessions during which rats learned to walk consistently for 5–10 min in both clockwise and counterclockwise directions at a relatively slow, speed (~3.3 m/min, 9 rotations per minute, RPM) with periods of resting between walking epochs. Walking was encouraged by the presence of a stationary paddle lowered to a point just above the track. At the end of the training, the rats were capable of walking steadily in both directions. All animals were also trained for the standard forelimb stepping test (Olsson et al., 1995).

2.3. Cannula and electrode implantation surgery

Rats were anesthetized with 75 mg/kg ketamine (Ketaved, Vedco, St. Joseph, MO) and 0.5 mg/kg medetomidine HCl, (Dexdomitor, Pfizer Animal Health, New York, NY) administered i.p. and placed in a stereotaxic frame (David Kopf Instruments, Tujunga, CA, USA) with heads fixed with atraumatic ear bars. The incision area was shaved and a long acting local anesthetic (1%, Polocaine, APP Pharmaceuticals, LLC, Schaumberg, IL) was injected along the intended incision lines. Ophthalmic ointment (Lacrilube, Akorn, Inc., Lake Forest, IL) was applied to prevent corneal dehydration and lidocaine gel was placed in

the ear canals. Small supplemental doses of ketamine were administered during the surgery as needed. A heating pad was used to maintain body temperature at 37°C.

Holes were drilled in the skull over the target recording sites in the left and right hemispheres. Electrode bundles were implanted unilaterally (left hemisphere) or bilaterally (left and right hemispheres) into the primary MCx (at coordinates: 2.0 mm anterior to bregma, 2.7 mm lateral from the sagittal suture and ventral 2.0 mm ventral from the skull surface) and SNpr (at coordinates: 3.2 mm anterior to the lambdoid suture, 2.2 mm lateral from the sagittal suture and 8.0 mm ventral from the skull surface). These bundles consisted of 8 stainless steel teflon-insulated 50 μm microwires plus an additional 9th wire with no insulation for ~1 mm on the recording tip serving as a local reference and an uninsulated ground wire which served as instrument ground (NB Labs, Denison, TX, USA). Microwires used for recordings had impedance of ~0.4 – 0.6 MΩ, in physiological saline at 135 Hz (nanoZ™ Impedance Tester, White Matter, LLC) with custom headstage adapter (Plexon, Dallas, TX, USA). Stainless steel guide cannulas (21-gauge, Plastics One, Roanoke, VA, USA) were implanted unilaterally into the left hemisphere or bilaterally into both hemispheres above the MFB for 6-OHDA or TTX infusion at coordinates: 4.4 mm anterior to the lambdoid suture, 1.2 mm lateral to sagittal suture and 6.3 mm ventral from the skull surface, 2 mm above the MFB to allow subsequent alignment of the 8.3 mm internal cannula. Bundles and guide cannula were secured to the skull with screws and dental cement (Ortho-Jet Liquid, Lang Dental Mfg. Co., Inc, Wheeling, IL) and the uninsulated ground wire from each set of electrodes was wrapped around a screw located in the skull bone above the cerebellum.

After completion of surgeries, ketoprofen (6 cc, 0.15% in 0.9% NaCl,) was administered subcutaneously, and atipamezole (0.3 mg/kg, sc) was administered to reverse the effect of medetomidine. The rat's recovery was monitored, and their diet was supplemented with fruits and bacon treats during the first week after the surgery.

2.4. 6-OHDA and TTX infusion procedure

The 22 rats (Groups 1–4) implanted with chronic recording electrodes and cannula for infusion of 6-OHDA or TTX into the MFB were allowed to recover for 7–9 days after electrode and cannula implantation surgery and acclimated to investigator handling. On the day of the 6-OHDA infusions (Day 0), control recordings of LFPs, neuronal spiking activity and behavioral tests were performed 30 minutes prior to intracerebral administration of 6-OHDA into the MFB. Desmethylimipramine HCl (30 mg/kg, i.p.) (Sigma-Aldrich Co.) was administered 10–20 min before the infusion of 6-OHDA to protect noradrenergic neurons. While the animals were awake and lightly restrained, 3 μl of a solution of 6-OHDA HBr (2 μg/μl) dissolved in 0.9% saline with 0.01% ascorbic acid were infused into the MFB via a 26-gauge stainless steel internal cannula. The internal cannula was attached to a 10 μl Hamilton micro syringe and inserted into the chronically implanted guide cannula with the tip protruding 2 mm below the end of the guide cannula. All injections were controlled by an electric pump (Harvard Apparatus, Holliston, MA, USA) and performed at a rate of 1 μl/min over 3 min. The cannula was left at the target site for 3 min after the infusion was completed. The efficacy of dopamine cell loss was assessed behaviorally using the stepping

test procedure at Day 1-Day 7 after the lesion (Olsson et al., 1995; Schallert and Tillerson, 1999). The extend of dopamine cell loss was assessed post-mortem using immunochemical staining for tyrosine hydroxylase (TH staining, see below).

The 3 rats (Group 4) implanted with chronic recording electrodes and cannula for infusion of TTX (Tocris Bioscience) were infused with TTX (0.3 μl of 50 μM TTX) instead of 6-OHDA.

Five rats (Group 6) received 6-OHDA infusions into the MFB at the same time during the electrode implantation surgery, at coordinates 4.4 mm anterior to the lambdoid suture, 1.2 mm lateral to sagittal suture and 8.3 mm ventral from the skull surface.

2.5. Drug treatment

Apomorphine (Sigma-Aldrich Co.) was injected at a dose of 0.075–0.1 mg/kg sc. Dopamine selective antagonists for D1 dopamine receptors (SCH-23390, Sigma-Aldrich, 0.2 mg/kg) and D2 dopamine receptors (eticlopride, Sigma-Aldrich Co., 0.3 mg/kg) were injected in combination (D1+D2 antagonists, sc) twice daily for 7 days: at 10:00 AM and at 5:00 PM.

2.6. Behavioral testing

Motor behavior was assessed using two different step-testing procedures – the standard forelimb stepping test (Olsson et al., 1995) and circular treadmill walking test (Avila et al., 2010). The treadmill consisted of a cylinder with a concentric inner solid core mounted on a rotating platform, providing a circular track 7 cm wide and 37 cm in circumference. A paddle was lowered over the track to encourage the rat to continue to walk to avoid being bumped as the treadmill turned. Sessions with treadmill walking were videotaped for off-line review. Step counts were taken before and after treatments with 6-OHDA, TTX or injection of dopamine receptor antagonists. Rats in groups with bilateral 6-OHDAinduced dopamine cell lesion and those treated with D1+D2 antagonists, were subjected to catalepsy testing. The treadmill was turned off within ~10 seconds if the rat remained immobile and began to be pushed by the paddle.

2.6.1. Standard forelimb stepping test—The stepping test was conducted daily before the recording sessions, and number of steps made by the *right forelimb* and by the *left forelimb* were counted. (Olsson et al., 1995). The number of steps made by the right paw (contralateral to the lesion) relative to the number made by the left paw (ipsilateral to the lesion) was calculated. Stepping tests were performed in the morning before 10 AM for both 6-OHDA lesioned rats and rats receiving D1+D2 antagonist injections.

2.6.2. Treadmill walking—To quantify the motor performance of the intact and DA-depleted rats during epochs of walking in a circular treadmill, the ratio of steps made by the inner hind paw relative to steps made by the outer hind paw was calculated over two 30 s epoch of consistent walking on the circular treadmill track in each direction (in/out ratios) (Brazhnik et al., 2014). Step ratios were only calculated for epochs of successful treadmill walking. After effective unilateral dopamine cell lesions, the hemiparkinsonian rats could make reasonable progress on the circular treadmill at a consistent speed of ~3.3

m/min (9 RPM) if they were oriented in the direction ipsilateral to the unilateral lesion, with their affected paws on the outside of the circular path. A successful treadmill walking trial consisted of walking on the circular treadmill for a continuous thirty second interval without stopping. If they were oriented in the opposite direction, contralateral to the lesion, they often failed to walk or reared up and tried to turn around. In this case, the treadmill was turned off after ~10 s of contact with the paddle and the trial was considered a failed trial. The percentage of completed 30 s trials (2 trials in each direction) was assessed. Rats were videotaped during each recording session. Rats with bilateral 6-OHDA lesion were placed in the rotating open cylinder without a paddle to encourage walking.

Treadmill walking tests were performed in the morning before 10 AM for both 6-OHDA lesioned rats and rats receiving D1+D2 antagonist injections. For rats receiving infusion of TTX into the MFB, treadmill walking was assessed hourly during recording sessions and forelimb stepping test was performed hourly after the first treatment with D1+D2 antagonists. Treadmill walking was also assessed before and 10–20 min after apomorphine administration.

2.6.3. Evaluation of catalepsy intensity—The degree of catalepsy was quantified with versions of the commonly used climbing grid test (Ahlenius and Hillegaart, 1986; Rodriguez et al., 2001) and standard bar test (Morelli and Di Chiara, 1985; Hoffman and Donovan, 1995; Molinet-Dronda et al., 2015). On Day 0 of D1+ D2 antagonist treatment, these two tests were performed before drug injection and hourly for 5–7 hours. On subsequent days, the tests were performed 1 h post-injection. The bar test was performed daily for bilaterally lesioned rats.

The *standard bar test* was performed by placing both forelimbs of the rat on a horizontal bar raised approximately 9–10 cm above the floor. The interval between placement of the forelimbs on the grid and the first complete removal of one of the paws from the support bar was recorded, with a cutoff time of 60 seconds. The *catalepsy grid test* utilized a stainless-steel wire grid oriented vertically at an angle of 45° to the floor surface (22 wide x 35 cm high with a 1.3-cm linear grid). The rats were placed on the grid with their heads facing toward the top of the grid. The time from the placement of the rat's paw on grid until the first movement of its paws toward the bottom of the grid was recorded, with a cutoff time of 60 sec.

The method for evaluation of the catalepsy strength was adopted with minor modifications from Molinet-Dronda et al. (Molinet-Dronda et al., 2015) and applied for both tests. The intensity of the cataleptic state was quantified by assigning a score for the duration of immobile episodes for each test up to 60 s. A score of 0 to 4 was assigned for each 60 s catalepsy test: 0 for catalepsy persisting 0–15 s; 1 for 16–30 s; 2 for 31–45 s; 3 for 46–60 s; or 4 for more than 60 s. Both tests were repeated four times at 4–5 min intervals, and the scores for each trial were summed. The maximal score possible for each set of tests was 16. For analysis of LFP and spike activity during severe akinesia in the hours following treatment with D1+D2 antagonists, recordings were taken during investigator-assisted movement. Investigator-assisted movement was defined as a period when the investigator held the rat so that the paws were in contact with the floor of the

cylinder and moved him slowly within the cylinder. This induced the rat to take stepping movements with his paws.

2.7. Electrophysiological recordings

Recordings of extracellular spike trains and LFP activity were initiated at 7–9 days post-surgery. Recordings of baseline activity for control data were performed during periods of treadmill walking on Day 0 at which point either infusions of 6-OHDA (Groups 1–3) or TTX (Group 4) were performed, or twice daily systemic injections of the D1+D2 antagonists (Group 5) were initiated. Recordings of baseline activity for rats receiving 6-OHDA infusion at the same time as electrode implantation (Group 6) were performed 7–9 days after surgery and before initiation of D1+D2 antagonist treatment on day 0.

After unilateral or bilateral injection of 6-OHDA into MFB (Groups 1 and 2), subsequent recordings were performed daily during the first week post-lesion, starting from 24 h (Day 1). In addition, early recordings were also performed in 7 rats (subset of Group 1) at 3 and 4 hours after 6-OHDA infusion on Day 0.

Recordings from rats with unilateral injection of 6-OHDA followed by apomorphine treatment (Group 3) on Day 1 (24 h) and Day 2 (48 h) post-lesion were obtained during treadmill walking,10–20 min after apomorphine injection.

Recordings from rats with TTX microinjections into the MFB (Group 4) were performed before the infusions and hourly from 1 to 5 h and at 24 h after TTX administration.

In rats undergoing 7 days of treatment with dopamine neuroleptics (Group 5), spike and LFP activity was recorded every morning during treadmill walking before the 10 AM injection of D1+D2 antagonists, approximately 18 h after the previous afternoon injection of antagonists (at 5 PM). For a subset of rats (n = 8) spike and LFP recordings were additionally performed hourly after the first injection of D1+D2 antagonists (Day 0) from 1 to 7 h post-treatment during investigator-assisted movement. Following the D1+D2 antagonist treatments, these rats were allowed a 7-day recovery period. Recordings were performed daily during the 7-day post-treatment recovery (recovery days R1-R7) following the last injection with D1+D2 antagonists.

In rats with 6-OHDA lesion that were treated with D1+D2 antagonists (Group 6), recordings were initiated at Day 7–9 post-surgery/post-lesion with the first injection of D1+D2 antagonists (Day 0) and performed on a daily basis during each of the 7-days of treatment with neuroleptics.

Extracellular spike trains and LFPs were amplified and filtered using Plexon pre-amplifiers (Dallas, TX, USA) and sampled with CED Micro1401 data acquisition interface systems (Cambridge Electronic Design, Cambridge, UK). Spikes and LFPs from signal wires were referenced to the 1 mm scraped 9th wire in the same bundle and all electrode bundles were referenced to instrument ground. Sampling rates were 40 kHz for spike trains and 1 kHz for LFPs. Action potentials were amplified (10,000x) and band-pass filtered (0.15–9 kHz). LFPs were amplified (1000x) and band-pass filtered (from either 0.7 or 1.7 high pass, to 170 or 300 for low pass Hz). Spike signals and LFPs recordings were digitized, stored and analyzed

offline using Spike2 software (Cambridge Electronic Design, see below). Motor activity was videotaped.

Data were collected during 2 epochs (each 300 s) of walking in the circular treadmill in both directions, or during 2 epochs of investigator-assisted movement during severe akinesia (1 to 7 hours after treatment with D1+D2 antagonists).

2.8. Data analysis

LFP and extracellular unit activity were analyzed using custom-written Spike2 and MATLAB scripts. Representative epochs 60 s in length and free of major artifacts were used to calculate LFP power during periods of walking on the circular treadmill.

Data from two electrodes per brain region and two epochs per behavioral state were obtained from each rat and averaged for analysis of power and coherence. As rats with left hemispheric lesions typically demonstrated difficulty walking in the direction contralateral to the lesion, data were taken only when rats were walking in the ipsilateral direction.

2.8.1. Spectral analysis of LFPs—For fast Fourier transfer (FFT)-based analysis of LFP power and MCx-SNpr coherence in the 29–55 Hz range, LFP recordings were smoothed to 500 Hz, and LFP power spectra and coherence (~1 Hz resolution) were obtained using a Spike2 script. The threshold for coherence significance was calculated for the averaged coherence spectra (Rosenberg et al., 1989). LFP ranges referred to as high beta/low gamma (HB/LG) in the current paper include spectra having peaks in the 29–40 Hz range, and mid-gamma as those having peaks between 41–55 Hz. Values for total power and mean coherence were summed or averaged, respectively, around dominant peaks (p) as $p \pm n$ Hz.

The Fourier spectra of LFP recordings can reflect elevated synchronous activity in one or more frequency ranges, as characterized by peaks in the power spectrum curve. We define the “peak frequency” as the frequency value corresponding to a peak in the power spectrum curve. A peak in a power spectrum was identified as „dominant” if it met three criteria, as illustrated in Supplementary Fig S1. First, it was larger than the values in the surrounding eight 1 Hz frequency bins (Doyle et al., 2005; Alonso-Frech et al., 2006). Second, the power spectrum slope changed sign from positive on one side of the peak to negative on the other side of the peak. Third, the curve surrounding the peak had a downward concavity, as indicated by the second derivative test. The frequency value corresponding to the dominant peak maximum is designated the “peak frequency” or “dominant peak” of that spectrum. The frequency values of the dominant spectral peaks were used to define ranges for calculating total power and mean coherence, as in Fig. 1D-F, and were plotted in box-and-whisker plots as in Fig. 1G.

Once the dominant peak frequency value was determined for a given epoch’s power spectrum, total LFP power or mean coherence was calculated for the 6 Hz range surrounding that frequency value. For total LFP power, this was performed by summing the areas of each of the six ~1 Hz spectra bins surrounding the peak in addition to the bin containing the dominant peak value itself. To calculate mean MCx-SNpr coherence in a given frequency

range, coherence spectrum values for the seven bins surrounding and including the peak were averaged. If there was no dominant peak in an epoch's power spectrum, the mean dominant peak frequency of the peak-containing spectra from rats in the same experimental group was used as the value for that spectrum for the purpose of calculating power and coherence. For this analysis, one dominant peak for each of the two frequency ranges was considered for each spectrum. If a spectrum had two peaks in a frequency range, the peak with the larger amplitude of the two was selected. Thus, the maximum number of dominant peaks per rat hemisphere for a given time point is eight and the maximum possible number of dominant peaks for a Group is n(hemispheres) × 8.

To visualize spectral power changes over time for the selected epochs, time-frequency wavelet spectra were constructed using continuous wavelet transforms. The Morlet wavelet was applied to the LFPs using 128 frequency scales and a time resolution of approximately 750 ms (Time-Frequency Toolbox (http:tftb.nongnu.org). Wavelet spectra were scaled to best show the high beta activity against minimum background noise. Coherence spectra were constructed using an FFT based analysis with a 10 s moving window (Chronux, http://chronux.org). The multitaper coherence analysis utilized 19 tapers, resulting in a bias of about 0.23 ($B = \frac{1}{\sqrt{v}}$, where B is the bias; ν is the degrees of freedom). To compensate for this, the smallest coherence value in the plot were adjusted to 0.23 and the largest to 1.23, rather than 0 and 1, respectively (Mitra & Bokil, 2008; personal communication).

2.8.2. Cell sorting and spike-triggered waveform analysis (STWA)—Rats which maintained stable signal-to-noise ratios in SNpr neuronal spiking activity over 7 days of recordings were considered for spike sorting and STWA analysis (5 rats with 6-OHDA-lesion and 8 rats with chronic D1+D2 antagonist treatment).

Recordings sampled at 40 kHz were high pass filtered at 300 Hz with a transition gap of 100 Hz to remove low frequency content. To establish a threshold for spike extraction, the signals were measured for root mean square amplitude and spike waveforms were identified and extracted when the amplitude of the signal exceeded 5 x root mean square threshold. Some rats were limited to 4 electrodes due to technical limitations. To further identify spike-like waveforms as components of ongoing spike trains, the unsorted spike waveforms were transformed using principal components analysis and clusters were identified using the normal mixtures clustering algorithm and used to create waveform templates. Interspike interval histograms were constructed from spikes conforming to individual templates and visually inspected for any spikes that occurred within 1 ms from each other to ensure effective templating. Spikes from for each epoch were then combined into multi-unit spike trains.

To assess the temporal relationship between the spiking activity of multiunit spike trains and LFP oscillations, spike triggered LFP waveform averages (STWA) were constructed using SNpr spike trains and both SNpr and MCx LFPs. Two 150 s of treadmill walking in the ipsilateral direction were used for each rat. For lesioned rats, data was from controls and days 1, 2 and 7 post-lesion. For rats treated with D1+D2 antagonists, data was from recordings taken on Day 1 and Day 7 before the 10 AM injections.

SNpr and MCx LFPs used for STWAs were band-pass filtered with a FIR filter (Spike2) using a 10 Hz range centered around the peak frequency observed in HB/LG LFP power for each rat at Day 7. Spikes were reference to LFP from the "neighboring" SNpr or MCx wire with the highest correlation to the wire used for the spike train.

Peak-to-trough amplitudes of the spike train triggered LFP waveform averages (STWAs) were obtained at or around the spike (zero time) and used as a measure of the synchronization of the spike trains to the dominant LFP oscillation. The interspike intervals in each multiunit spike train was then shuffled 100 times and each shuffled spike train was used to create a STWA, each of which was measured for the peak-to-trough amplitude. Spikes were considered to have a preferred phase relationship with the filtered LFP when the peak-to-trough amplitude of the unshuffled spike train STWA was greater than the averaged shuffled STWA amplitude plus three standard deviations of the mean. Both the proportion of significantly correlated spike trains and the mean unshuffled:shuffled STWA ratio were reported as measures of change in the spike-LFP relationships for SNpr and MCx following lesion and dopamine antagonist treatment. Representative examples of this analysis showing individual STWAs with the mean amplitude of the distribution of 100 STWAs generated from shuffled spike trains are depicted in Fig. S2A.

Data from the spike-train-LFP analysis were processed in two ways. First, the percentage of spike trains that were significantly correlated with SNpr and MCx LFP oscillations was calculated for epochs from before and after the onset of dopamine cell lesion (Day 0 and post-6-OHDA: Day 1, Day 2 and Day 7 post-lesion) or chronic blockade of dopamine receptors in D1+D2 antagonist treated rats (next morning after 7 days of treatment with D1+D2 antagonists). Second, to assess the overall extent of phase-locking of the SNpr neurons in the control vs. DA-deprived rats (post-6-OHDA lesion or treated with D1+D2 antagonists), mean ratios of unshuffled/shuffled peak-to-trough amplitudes for spike trains were obtained.

2.9. Statistical analysis

Changes in LFP power and coherence, STWA ratios, and behavioral test results over multiple points in time were analyzed using one- or two-way repeated measures (RM) analysis of variance (ANOVA) with *post hoc* comparisons. Holm-Sidak *post hoc* test was used to detect significant differences between groups. In cases where the data did not meet the assumptions of normal distribution and/or equal variance, Friedman Repeated Measures ANOVAs with Dunn's *post hoc* comparisons were used. For comparisons of two groups of variables, paired t-test or Wilcoxon signed-rank tests were applied. Differences in the proportions of significantly correlated neurons were evaluated with chi-square tests.

Results analyzed with parametric tests are presented as the mean value ± standard error of the mean (SEM), unless otherwise indicated. Spectral peak and STWA data are presented in box plots depicting the median values and the 25^{th}-to-75^{th} quartile range. For statistical analysis of spectral peaks, the maximum value of N is determined by the number of rats × 2 electrodes per recording region × 2 epochs per rat and between 0 and 2 dominant peaks per spectrum. Thus, in a group of 9 rats (15 hemispheres total for LFP recordings), such as in Fig. 3, the maximum value of N for an ANOVA test would be 120 = 15 × 2 × 2 × 2. For

statistical analysis of STWA ratios and the percentage of significantly correlated STWAs, the value of N is the total number of spike trains analyzed across all rats. Two epochs of spiking activity were analyzed for each rat. For the spiking data from the group of 5 rats shown in Fig. 1, the value of n for a one way RM ANOVA test was 64 = 2 × (4 + 4 + 8 + 8 + 8), as two rats contributed spike trains from 4 electrodes and three rats contributed spike trains from 8 electrodes.

All statistical analysis was performed with SigmaPlot 12.1 (SyStat Software, San Jose, CA, USA) with a level of significance of $\alpha = 0.05$.

2.10. Histology

Rats were deeply anesthetized and recording sites were marked by electrolytic lesions. Rats were perfused intracardially with 200 ml cold saline followed by 200 ml 4% paraformaldehyde in phosphate buffer solution. Fixed brains were sliced and 40 μm coronal sections containing the substantia nigra pars compacta (SNpc) were immunostained for tyrosine hydroxylase (primary rabbit polyclonal anti-TH antibody,1:200 dilution; Pel-Freez Biologicals, and biotinylated anti-rabbit IgG secondary antibody, 1:200 dilution; Vector Labs). The staining was processed using avidin-biotin-perioxidase complex (ABC kit; Vector Labs) and 0.05% 3,3'-diaminobenzidine tetrahydrochloride with 0.01% H2O2 (DAB kit, Vector Labs). ImageJ software (NIH) was used to evaluate the extent of tyrosine hydroxylase staining in anterior, middle and posterior sections of the substantia nigra and ventral tegmental area. Severe loss of tyrosine hydroxylase stained-neurons and fibers in the substantia nigra (more than 95%) and partial loss of dopamine neurons and fibers in the lateral ventral tegmental area (~15%) was observed in the dopamine lesioned hemisphere. To verify electrode bundle placement, the coronal sections were counterstained with cresyl violet and 5% potassium ferricyanide/9% HCl to reveal iron disposition marking the location of the electrode tips.

3. Results

3.1. Unilateral 6-OHDA-induced dopamine lesion days 1–7: changes in MCx and SNpr LFP peak frequency, power, coherence and spike synchronization

To probe relationships between early changes in motor circuits triggered by dopamine cell lesion and the emergence of parkinsonian motor symptoms, spike and LFP activity was recorded from the MCx and SNpr each day over the week immediately following unilateral injection of 6-OHDA into the MFB. Recordings were performed on rats trained to walk on a rotating circular treadmill. Continuous walking was encouraged by the presence of a paddle lowered to a point just above the track (see methods). This task provides a relatively stable behavioral state which allows for quantification of motor deficits as rats with unilateral dopamine cell lesions could walk consistently in a circular treadmill when oriented in the direction ipsilateral to the lesion but typically showed less consistent progress in the contralateral direction (Avila et al., 2010; Brazhnik et al., 2012). Thus, following unilateral injection of 6-OHDA, recordings were obtained from the lesioned hemisphere as rats walked ipsilateral to the lesion.

Figure 1 shows the time course of changes in MCx and SNpr LFP power and MCx-SNpr LFP coherence in the lesioned hemisphere, as well as the frequencies of dominant peaks in these LFP spectra, and spike-local field relationships (STWAs) over 7 a day period, during ipsilateral treadmill walking, starting the first day (Day 1) after MFB injections of 6-OHDA (Fig 1 A-I). LFP analysis was focused on the 29–40 Hz high beta/low gamma (HB/LG) and the 41–55 Hz mid-gamma ranges. Measures of stepping activity and gait were obtained as rats were oriented to walk both ipsilaterally and contralaterally, relative to the lesion (Fig. 1 J-L).

In the MCx, prior to 6-OHDA MFB infusion, FFT-based analysis of LFP in MCx revealed modest dominant peaks (see methods) in the power spectra in the mid-gamma range during treadmill walking as shown in Fig. 1A, D and red box plots in G. The median peak frequency of the dominant peaks in the MCx LFP spectra in these control recordings was 43.0 Hz (interquartile range (IQR): 38.3–44.9 Hz, n = 44, Fig. 1G). Following injection of 6-OHDA, there was a shift in the frequencies of the dominant peaks in MCx LFPs within the 29 to 55 Hz range from mid-gamma (40–55 Hz) in control down to the HB/LG (29–40 Hz) range across all days ($p < 0.001$, $H = 62.817$, $df = 4$, ANOVA on Ranks, Fig. 1G). By Day 1 following 6-OHDA injection, the median frequency of the dominant MCx LFP peaks in the lesioned hemisphere fell, albeit not significantly ($p > 0.05$, $Q = 2.391$, $n = 35$, Dunn's *post hoc*), relative to control, to 36.1 Hz (IQR: 33.2–40.0 Hz), and by Day 3 the median peak frequency was 32.2 Hz (IQR: 32.2–34.2 Hz), significantly lower than in control recordings ($p < 0.05$, $Q = 4.901$, $n = 28$, Dunn's *post hoc*). On Days 5–7 post-lesion, the frequencies of the MCx LFP spectral peaks stabilized around 31–32 Hz (Day 5 median: 31.3 Hz, IQR: 30.2–32.2 Hz, $p < 0.05$, $Q = 6.451$, $n = 27$; Day 7 median: 32.2 Hz, IQR: 30.2–33.7 Hz, $p < 0.05$, $Q = 6.052$, $n = 33$, Dunn's *post hoc*). The relatively rapid loss of the mid-gamma peaks in the MCx, and subsequent emergence of dominant peaks in the high beta range is displayed in box plots in Fig. 1G showing the median and 25–75% range of the individual peak frequencies.

As the frequencies of the dominant peaks in the 29–55 Hz range during treadmill walking shifted downward, from medians of ~43 Hz in the control state to ~31–32 Hz one week after dopamine cell lesion, total LFP power around the dominant spectral peaks in the HB/LG (29–40 Hz) range (peak +/− 3 Hz, Fig. 1D, red bars) increased significantly ($p < 0.001$, $F_{(7,56)} = 7.82$, $n = 9$ rats, one way RM ANOVA); in a manner positively and linearly correlated with time post-lesion ($p < 0.001$, $R^2 = 0.94$, $F_{(1,6)} = 91.224$, $n = 8$ days, linear regression). By Day 4 post-lesion, total power in this range in the lesioned hemisphere was significantly greater than LFP power in the same frequency ranges in control recordings (Day 4: 2.74×10^{-5} vs. 6.28×10^{-6} mV^2, $p = 0.035$, $t = 2.709$, Holm-Sidak *post hoc*).

Unilateral dopamine cell lesion also induced changes in SNpr LFP peak frequency and power in the lesioned hemisphere. In the SNpr, before 6-OHDA lesion, SNpr LFP recordings during treadmill walking, like those from the MCx, showed more dominant peaks in power spectra in the mid-gamma range than in the HB/LG range (Fig. 1G). The dominant peaks in the SNpr power spectra in control recordings exhibited a median frequency in the 29–55 Hz range of 46.9 Hz (IQR: 40.0–51.8 Hz, n = 15), but were relatively modest and broadly distributed and thus not evident in the averaged spectra (Fig 1E).

Fig. 1G shows that following the 6-OHDA lesion, dominant peaks in the SNpr (blue box plots) in the lesioned hemisphere began to cluster at a frequency in the HB/LG range significantly lower than in control recordings ($p < 0.001$, $H = 35.076$, $df = 4$, ANOVA on Ranks). On Day 3 post-lesion the median dominant peak frequency was 29.8 Hz (IQR: 29.3–32.2 Hz) which was significantly lower than in control recordings ($p < 0.05$, $Q = 4.804$, $n = 12$, Dunn's *post hoc*) and remained consistently observed in the high beta 29–35 Hz range through Days 5 and 7. SNpr LFP total power around the dominant peaks in the HB/LG range increased after 6-OHDA injection, over a time frame similar to that observed in the MCx (Fig. 1E, blue bars, $p < 0.001$, $F_{(7,56)} = 5.31$, $n = 9$ rats, one way RM ANOVA), with significant increases by Day 6 ($t = 3.135$, $p = 0.016$, Holm-Sidak *post hoc)*. These gradual increases in SNpr power are evident in wavelet based spectrograms (Fig. 1B) and in LFP power spectra (Fig. 1E) in the HB/LG range through Day 7 post-lesion, and are positively and linearly correlated with time post-lesion ($p < 0.001$, $R^2 = 0.95$, $F_{(1,6)} = 109.002$, $n = 8$ days).

6-OHDA induced dopamine cell lesion was also associated with early increases in MCx-SNpr coherence and synchronization of SNpr spiking. Notably, significant increases in MCx-SNpr LFP coherence in the HB/LG range emerged more rapidly after dopamine cell lesion than increases in LFP spectral power in either area. This can be observed in the coherence time-frequency plots (Fig. 1C), coherence spectra (Fig. 1F, mean coherence bar graphs) and distribution of dominant peaks in the LFP spectra (Fig. 1G). MCx-SNpr LFP coherence spectra, prior to 6-OHDA lesion, exhibited dominant peaks (see methods) with a median frequency of 40.0 Hz (IQR: 37.1–41.5 Hz, $n = 17$) in recordings during treadmill walking before lesion. Following unilateral 6-OHDA lesion, the median peak frequency of dominant peaks in the coherence spectra became significantly lower ($p < 0.001$, $H = 33.288$, $df = 4$, ANOVA on Ranks) as soon as Day 1 post-lesion ($p < 0.05$, $Q = 3.486$, $n = 29$, Dunn's post hoc) and remained significantly lower through Day 7 (Fig. 1G, gray box plots).

Comparisons of mean coherence around the peak frequencies (peak +/− 3 Hz, Fig. 1F inset, bar graph), show mean coherence is both positively correlated with time post-lesion ($p < 0.001$, $R^2 = 0.99$, $F_{(1,6)} = 836.76$, $n = 8$ days) and significantly increased relative to control ($p < 0.001$, $F_{(7,56)} = 47.07$, $n = 9$ rats, one way RM ANOVA) as early as Day 1 post-lesion ($p = 0.011$, $t = 2.63$, Holm-Sidak *post hoc*), in contrast to the significant changes in LFP power which emerge relatively later on Day 4 in MCx and Day 6 in SNpr. These results argue that the gradual increases in LFP power in the high beta range in MCx and SNpr reflect an early alignment in patterned activity in this frequency range involving components of the basal ganglia impacting the MCx and SNpr. Identifying those components remains to be accomplished for the rat PD model, although studies in mice provide insight (Willard et al., 2019; Kovaleski et al., 2020).

To further examine the functional significance of the coherent LFP changes in MCx and SNpr over the first week post-lesion, we sought to determine whether the increases in HB/LG LFP power observed in SNpr during treadmill walking correlate with changes in spike timing in this area. To this end, we examined phase-relationships between SNpr spikes and simultaneously recorded LFPs in SNpr and MCx on Day 1, Day 2 and Day 7 post-lesion ($n = 64$ spike trains, 5 rats; see methods for details). While mean multiunit spike rates were

not significantly different over time postlesion relative to controls in this data set (Fig S2D), it should be noted that this result cannot be taken to indicate that single unit SNpr firing rates were unaltered in this PD model, as the number of units participating in the multi-unit spike trains could be variable. That being said, it is clear that the timing of the spikes in the multiunit spike trains was altered post-lesion. In parallel with the increases in SNpr LFP power in the HB/LG range in the dopamine cell-lesioned hemisphere during treadmill walking, increases were also observed in the phase locking of SNpr spikes in multi-unit spike trains to SNpr and MCx LFP oscillations in the HB/LG range. Spike-LFP phase locking was significantly increased by Day 2, and more exaggerated by Day 7 post-lesion (Fig. 1H, I), as reflected in the unshuffled-to-shuffled peak-to-trough STWA amplitude ratios (Fig. 1H) for both SNpr-spike-to-MCx-LFP STWAs (red boxes, $p = 0.003$, $X^2 = 14.04$, df = 3, n = 5 rats, RM ANOVA on Ranks; Day 2: $p < 0.05$, $q' = 2.85$; Day 7: $p < 0.05$, $q' = 4.43$, Dunnett's *post hoc*) and for SNpr-spike-toSNpr-LFP STWAs (blue boxes, $p = 0.003$, $X^2 = 14.04$, df = 3, n = 5 rats, RM ANOVA on Ranks; Day 2: $p < 0.05$, $q' = 2.85$; Day 7: $p < 0.05$, $q' = 4.74$, Dunnett's *post hoc*). Increases in spike synchronization and phase-locking was also evidenced by increases in the proportion of spikes in the SNpr multiunit spike trains (Fig. 1I) that were significantly correlated with the MCx LFPs (red boxes, $p < 0.001$, $F_{(3,12)} = 58.653$, n = 5 rats, one way RM ANOVA; Day 2: $p = 0.003$, $t = 4.282$; Day 7: $p < 0.001$, $t = 12.132$, Holm-Sidak *post hoc*) and the proportion of SNpr spikes significantly correlated with SNpr LFPs (blue boxes, $p < 0.001$, $F_{(3,12)} = 35.495$, n = 5 rats, one way RM ANOVA; Day 2: $p = 0.018$, $t = 3.326$; Day 7: $p < 0.001$, $t = 9.832$, Holm-Sidak *post hoc*). The timing of the multiunit SNpr spikes became more focused on a narrow phase of the dominant LFP oscillation over time (Fig S2B). Prior to lesion, SNpr spikes showed a modest phase preference to SNpr LFPs ($z = 8.36$, Rayleigh test, $p<0.05$) and no phase preference to MCx LFPs ($z = 3.37$, Rayleigh test). Following lesion, spikes began showing significant phase preference to both SNpr and MCx LFPs with the preference becoming stronger on each successive day. Mean preferred phase angles were significantly different from control in SNpr-SNpr spike-LFP STWAs at days 2 and 7 and in MCx-SNpr spike-LFP STWAs at days 1, 2, and 7 as indicated by Mardia-Watson-Wheeler test, (Fig. S2).

Collectively, these data show that spiking in basal ganglia output neurons becomes significantly correlated with dominant peaks in the HB/LG LFP activity in MCx and SNpr during treadmill walking in the lesioned hemisphere by the second day post-lesion. Thus, the changes in firing patterns and network function supporting the emergence of synchronized and oscillatory high beta activity throughout these motor circuits begin soon after lesion and continue to evolve over the first week post-lesion.

3.2 6-OHDA lesion-induced changes in motor behavior

In marked contrast to the gradual ramping up of LFP power over the days post-lesion during treadmill walking, unilateral motor dysfunction emerged quickly. The data in Fig. 1 show that dramatic impairment of motor function emerged within 24 hours post-lesion and persisted over the first week, as indicated by 3 different measures. First, by Day 1 post-lesion, and through Day 7, the forelimb step test (Fig. 1J) showed a dramatic and persistent decrease in the number of steps made by the affected paw (contralateral to the

dopamine lesioned hemisphere) relative to steps made by the intact paw (ipsilateral to the lesion) ($p < 0.001$, $X^2 = 36.380$, df = 7, n = 10 rats, RM ANOVA on ranks; Day 1: $p < 0.05$, Q = 3.062; Day 7: $p < 0.05$, Q = 3.572, Dunn's *post hoc*).

Second, in/out step ratios of hind paw stepping during treadmill walking in the direction contralateral to the lesioned hemisphere (Fig. 1K) were significantly altered relative to control ($p < 0.001$, $F_{(7,31)} = 8.268$, n = 10 rats, one way RM ANOVA) on Day 1 post-lesion ($p < 0.001$, t = 6.033, Holm-Sidak *post hoc*), with the degree of impairment similar to that seen on Day 7 post-lesion ($p < 0.001$, t = 6.229, Holm-Sidak *post hoc;* Day 1 vs Day 7, p = 0.997, t = 0.977).

Third, the proportion of completed trials (walking for at least 30 s) decreased to 50% on Day 1 (from 100% in control) when the lesioned rats were oriented in the circular treadmill in the direction contralateral to the lesion (Fig. 1L). This decrease remained stable over seven post-lesion days (45–55%), suggesting no further decline in the ability to walk in the contralateral direction on the circular treadmill over this time period.

Overall, these results show that the motor deficit induced by dopamine cell loss has a rapid onset, with decreased LFP activity and dominant peak frequencies in mid-gamma ranges in MCx also evident quite early. Notably, increases in coherence of SNpr LFPs and spikes with MCx LFPs, and progressive and dramatic increases in HB/LG MCx and SNpr LFP total power in the high beta range emerge over subsequent days post-lesion but were not associated with evidence of a further progression in severity of motor dysfunction over that time period.

3.3. Bilateral 6-OHDA-induced dopamine cell lesion: Days 1–7changes in MCx and SNpr LFP activity

The effects of bilateral lesion of nigral dopamine neurons were examined in 3 rats (5 total hemispheres) to determine whether the exaggerated oscillatory activity would emerge more rapidly following bilateral dopamine cell loss (Fig. 2). In fact, the results showed the time frame for changes in the bilaterally lesioned rats appeared similar to that observed in unilaterally lesioned rats

Following bilateral lesion, rats were unable to walk effectively in the treadmill at the normal rotation speed. Rather than utilizing the circular treadmill for these rats, LFP activity from 5 hemispheres was acquired during intermittent epochs of walking in both directions when the rats were placed inside a plexiglass open cylinder rotated at low speed (5 RPM instead of standard 9 RPM). During these intermittent epochs of walking, MCx and SNpr LFP power around the dominant peaks in the HB/LG range (peak +/− 3 Hz) was positively and linearly correlated with the elapsed time post-lesion (MCx: $p < 0.001$, $R^2 = 0.98$, $F_{(1,6)} = 284.575$; SNpr: $p = 0.001$, $R^2 = 0.85$, $F_{(1,6)} = 33.635$), over 7 days post-lesion, similar to observations from the unilaterally lesioned rats. The total power in the MCx (Fig. 2A) and SNpr (Fig. 2B) became significantly greater over time post-lesion, relative to total power in the same frequency range in control recordings (MCx: $p < 0.001$, $F_{(7,28)} = 6.658$, n = 5; SNpr: $p = 0.002$, $F_{(7,28)} = 4.593$, one way RM ANOVA), on post-lesion Day 4 (MCx: p = 0.018, t = 3.089, Holm-Sidak *post* hoc) and Day 7 (SNpr: $p < 0.001$, t = 4.498, Holm-Sidak,

post hoc), respectively. MCx-SNpr coherence spectra (Fig. 2C) also showed significantly increased mean coherence around the coherence peaks ($p < 0.001$, $F_{(7,28)} = 23.484$, one way RM ANOVA) on post-lesion Day 3 ($p = 0.001$, $t = 4.084$, Holm-Sidak *post hoc*).

The bilaterally lesioned rats also showed early decreases in the median frequency of MCx LFP dominant peaks closely resembling those observed in the lesioned hemisphere of the unilaterally lesioned rats. Before 6-OHDA bilateral lesion, the median peak frequency in the 29–55 Hz range in the MCx LFP power spectra during treadmill walking (Fig. 2D, red box plots) was 44.0 Hz (IQR: 39.1–47.6 Hz, n = 20). After the bilateral 6-OHDA lesion, the median frequency became significantly lower on all subsequent days ($p < 0.001$, $H = 52.182$, $df = 4$, n = 5 hemispheres in 3 rats, ANOVA on ranks), including Day 1 ($p < 0.05$, $Q = 3.455$, n = 20, Dunn's *post hoc*) when the median peak frequency in the MCx was 35.2 Hz (IQR: 33.2–37.1 Hz).

In the SNpr, prior to 6-OHDA lesion, power spectra exhibited dominant peaks with a median peak frequency of 40.0 Hz (IQR: 35.6 – 46.9 Hz, n = 13) (Fig 2D, blue box plots). Following lesion, the median of dominant peaks became significantly lower ($p < 0.001$, $H = 33.684$, $df = 4$, ANOVA on Ranks) on Day 3 ($p < 0.05$, $Q = 4.640$, n = 9, Dunn's *post hoc*). Similarly, before bilateral 6-OHDA lesion, MCx-SNpr coherence spectra (Fig 2D, grey box plots) exhibited dominant peaks with a median peak frequency of 50.8 Hz (IQR: 39.8–53.0 Hz, n = 4); and following lesion, the median of dominant peaks became significantly lower ($p < 0.001$, $H = 21.446$, $df = 4$, ANOVA on Ranks) on Day 1 ($p < 0.05$, $Q = 2.634$, n = 13, Dunn's *post hoc*).

3.4 Bilateral 6-OHDA-induced changes in motor function

The rats with bilateral loss of dopamine in the BG also exhibited a rapid onset of severe motor deficits bilaterally. This was evident by Day 1, 24 hours after bilateral dopamine cell lesion, as shown in Fig. 2E-G, before appearance of significant increases in LFP power in HB/LG activity in the MCx and SNpr. All three animals with bilateral lesions could make only a few steps with either left or right paws in the standard forelimb stepping test (Fig. 2F) showing a significant difference from control state ($p < 0.001$, $F_{(2,8)} = 131.435$, n = 3, two way RM ANOVA) by Day 1, 24 hours post-lesion (left paw: $p < 0.001$, $t = 17.053$; right paw: $p < 0.001$, $t = 15.263$, Holm-Sidak *post hoc*). The motor deficit was persistent over the following 6 days ($p = 0.389$). Motor impairment was also quantified by the bar test (Fig. 2E).

These results support the view that the sequence of changes in motor circuit LFP activity in a given hemisphere following ipsilateral dopamine cell lesion is not substantially impacted by whether or not the contralateral hemisphere is also lesioned. Motor symptoms emerge earlier in conjunction with reduction in mid-gamma MCx LFP activity and remain robust over 7 days post-lesion while SNpr LFP and spike synchronization and MCx and SNpr LFP power in the HB/LG range show gradual increases.

3.5. Chronic dopamine receptor blockade with D1+D2 antagonists: Days 1–7 changes in MCx and SNpr LFP power, coherence and spiking activity

It has been previously shown, somewhat problematically, that although acute treatment with dopamine receptor antagonists induces catalepsy, this rapidly emerging catalepsy does not appear to be associated with the presence of beta range oscillatory activity in the rat motor cortex (Mallet et al., 2008; Degos et al., 2009). However, as exaggerated high beta range LFP synchronization in motor cortex and basal ganglia circuits in dopamine-depleted rats appears to be highly state-dependent (Avila et al., 2010; Brazhnik et al., 2012; Brazhnik et al., 2014; Delaville et al., 2014), it seemed possible that such synchrony is not evident in the cataleptic rats due to their behavioral state. Moreover, the observations described above suggest that it takes several days for exaggerated beta range LFP power to fully emerge after dopamine cell lesion. Taking into consideration that the emergence of synchronized beta range activity could be both a state- and time-dependent phenomenon, we hypothesized that increases in beta range activity would be evident in recordings from rats after several days of neuroleptic treatment, when they emerge from catalepsy and can engage in treadmill walking. Moreover, it seemed possible these plasticity-dependent changes in circuit function might remain in place for a period of days after the chronic treatment was discontinued.

To explore this, a protocol was developed involving twice daily injections of a combination of the D1 and D2 dopamine receptor antagonists, SCH 23390 and eticlopride (D1+D2 antagonist, s.c.) for a period of 7 days. First, rats (n = 10 rats, total 16 hemispheres, see methods) were implanted with electrode bundles in the MCx and SNpr and allowed to recover for 7–9 days. They then received antagonist treatment twice a day, at 10 AM and 5 PM, for 7 days. This was followed by a 7 day wash out period. MCx and SNpr activity was recorded each day during treadmill walking in the morning prior to that day's first injection, following an 18 h period for recovery from catalepsy from the previous day's 5 PM injection (Fig. 3). These experiments were performed to determine whether chronic neuroleptic-induced dopamine receptor blockade would induce changes in MCx and SNpr LFP properties or patterns at a time point after drug treatment when the rats were able to complete treadmill walking trials effectively.

Results showed that chronic D1 + D2 antagonist treatment induces increases in MCx and SNpr LFP power and coherence. Recordings of LFP activity were obtained from 9 rats (n = 15 hemispheres total). As observed following dopamine cell lesion, chronic dopamine receptor blockade was also associated with both early and more gradual changes in MCx and SNpr LFP patterns. Chronic D1+D2 antagonist treatment induced an early shift in peak frequency values in MCx and SNpr LFP power spectra and in MCx-SNpr coherence spectra. Relatively more gradual increases in oscillatory LFP activity in the MCx and SNpr were evident during treadmill walking after the rat had recovered from catalepsy associated with the previous 5 PM treatment. Recordings obtained during treadmill walking in the morning before injection of D1 + D2 antagonist showed oscillatory LFP activity in the HB/LG frequency range emerged gradually in the SNpr and MCx along with increases in MCx-SNpr coherence over the 7-day regimen.

This can be seen in the wavelet-based spectrograms (Fig. 3 A-C), MCx and SNpr spectral power and MCx-SNpr coherence (Fig. 3 D-F, line graphs and bar graphs, inset). As was

observed following dopamine cell lesion, LFP power and coherence in the HB/LG range increased in a linear manner over the 7 days of chronic D1+D2 antagonist treatment (MCx: $R^2 = 0.90$, $p < 0.001$, $F_{(1,6)} = 56.288$; SNpr: $R^2 = 0.94$, $p < 0.001$, $F_{(1,6)} = 89.962$; MCx-SNpr coherence: $R^2 = 0.95$, $p < 0.001$, $F_{(1,6)} = 118.472$, linear regression, see Fig. 1A-F). Significant increases in MCx LFP total power in the HB/LG frequency range ($p < 0.001$, $F_{(7,98)} = 7.749$, n = 15, one way RM ANOVA) were evident on Day 2 ($p = 0.034$, $t = 2.680$, Holm-Sidak *post hoc*), and in the SNpr-MCx coherence ($p < 0.001$, $F_{(7,98)} = 16.034$, one way RM ANOVA) on Day 1 ($p = 0.027$, $t = 2.250$, Holm-Sidak *post hoc*) during treadmill walking (~18h after PM treatment with D1+D2 ant), while increases in the SNpr LFP total power display variability, becoming significant ($p < 0.001$, $F_{(7,98)} = 10.342$, one way RM ANOVA) only on Day 5 ($p = 0.002$, $t = 3.612$, Holm-Sidak *post hoc*).

Recordings from the MCx and SNpr before D1+D2 antagonist treatment show dominant spectral peaks (Fig. 3G) in MCx LFP total power, SNpr LFP total power and in MCx-SNpr coherence within the 29–55 Hz range with median frequencies of 41.0 Hz (IQR: 36.1–46.6, n = 68), 38.1 Hz (IQR: 35.2–44.9, n = 25) and 39.1 Hz (IQR: 36.1–44.9, n = 34), respectively. After initiation of daily treatment with D1+D2 antagonists, the median peak frequencies became significantly lower in the MCx ($p < 0.001$, $H = 24.133$, ANOVA on ranks), SNpr ($p < 0.001$, $H = 20.662$, ANOVA on Ranks), and in MCx-SNpr coherence spectra ($p = 0.002$, $H = 17.250$, ANOVA on ranks). By Day 1 of treatment with D1+D2 antagonist, the median frequency of dominant peaks was significantly decreased, relative to the pre-treated state, in the MCx LFP spectra (37.1 Hz, $p < 0.05$, $Q = 2.563$, n = 70, Dunn's *post hoc*) and in MCx-SNpr coherence spectra (36.6 Hz, $p < 0.05$, $Q = 2.938$, n = 52, Dunn's *post hoc*). The median peak frequency in the SNpr became significantly lower on Day 5 of treatment (33.2 Hz, $p < 0.05$, $Q = 4.130$, n = 38, Dunn's *post hoc*). Over the consecutive 7 days of treatment, the spectral peaks in the MCx LFP power and MCx-SNpr coherence exhibited greater variability than that following 6-OHDA-induced DA cell lesion, while their median values were similar in the HB/LG range. This may have been due to the intermittent nature of the receptor blockade.

Recovery of the MCx and SNpr LFP activity from the effects of chronic blockade of DA receptors was observed over a period of 7 days after the last PM injection of D1+D2 antagonists (data not shown). Small, but significant, increases in the MCx and SNpr LFP power and coherence in the beta frequency range were still detected during treadmill walking 42 h after last PM treatment (R1, $p < 0.05$). Collectively, by Day 3 and Day 5 after cessation of chronic D1+D2 antagonist treatment, the mean LFP power and MCx-SNpr coherence in the HB/LG frequency range and the frequency of the dominant spectral peaks were not different from those in control ($p > 0.05$, n = 11 hemispheres).

D1+D2 antagonist treatment also induced increased synchronization of SNpr spiking activity. As seen after dopamine cell lesion, increases in LFP power during treadmill walking in the high beta frequency range in SNpr and MCx LFP and SNpr-MCx coherence following 7 days of chronic D1+D2 antagonist treatment were clearly associated with increased phase-locking of spikes to LFP oscillations in the same frequency range. The SNpr multi-unit spike trains (n = 144 spike trains, 10 hemispheres) at Day 7 of chronic blockade of dopamine receptors exhibited significantly greater spike-LFP phase-locking than in the

control condition. This was evident from both the increased unshuffled-to-shuffled peak-to-trough STWA amplitude ratios (Fig. 3H) for SNpr spike to MCx LFP STWAs (red boxes, $p = 0.002$, $Z = 2.803$, Wilcoxon signed-rank test) and SNpr spikes to SNpr LFPs (blue boxes, $p=0.002$, $Z = 2.803$ Wilcoxon signed-rank test), and the increased proportion of spike trains significantly correlated with the SNpr (blue boxes, $p = 0.002$, $Z = 2.812$, Wilcoxon signed-rank test) and MCx LFP (red boxes, $p = 0.001$, $t = 11.665$, $df = 9$, paired t-test). This is consistent with previous observations of increased phase-locking of spiking activity in the SNpr after 6-OHDA-induced dopamine cell-lesion (Brazhnik et al., 2012; Brazhnik et al., 2016) and this study - Fig. 1H, I). Moreover, as shown in Fig. S2C, a phase distribution analysis of multiunit spike trains showed changes following D1+D2 antagonist treatment. Prior to D1+D2 antagonist treatment, SNpr spikes exhibited mild preferred phase angles for both SNpr LFPs ($z = 25.11$, Rayleigh test, $p<0.05$) and MCx LFPs ($z = 34.92$, Rayleigh test, $p < 0.05$). While the averaged multi-unit spike-train firing rates /channel were not different at Day 7 after chronic blockade with D1+D2 antagonists relative to the control state ($p = 0.481$, paired t-test (Fig S2D), on Day 7 following treatment SNpr spikes became more strongly concentrated around their preferred phase angle for both SNpr LFPs ($z = 86.89$, Rayleigh test) and MCx LFPs ($z = 84.17$, Rayleigh test, $p < 0.05$). Mean preferred phase angles for SNpr spike trains were also significantly different at Day 7 relative to control for both SNpr LFPs (82.56° vs. 116.2°, $W = 57.5$, Mardia-Watson-Wheeler test, $p < 0.05$) and MCx LFPs (86.02° vs. 108.2°, $W = 43.6$, $p < 0.05$).

3.6 D1+D2 antagonist-induced changes in motor behavior

Rats expressed profound catalepsy in the hours immediately following D1+D2 antagonist treatment (Fig. 5K). The following morning (18 hours after the previous day's 5 pm treatment) rats were capable of walking on the circular treadmill, although performance in the forelimb stepping test was substantially reduced and remained significantly depressed, over the 7 day regimen (Fig. 3J, $p = 0.006$, $F_{(1,49)} = 15.488$, $n = 8$ rats, two way RM ANOVA; Day 1: $p < 0.001$, $t = 9.009$, Holm-Sidak *post hoc*). However, the rats demonstrated linear improvement in the forepaw step test over the 7 day regimen (left paw: $R^2 = 0.93$ $p < 0.001$, $F_{(1,5)} = 67.652$; right paw: $R^2 = 0.880$ $p = 0.002$, $F_{(1,5)} = 36.596$, linear regression). Indeed, the rats were able to walk steadily on the treadmill in each direction without notable difficulties on days 1–7 post-treatment (Fig. 3K, L, $p = 0.546$, $F_{(1,53)} = 0.397$, $n =10$ rats, two way RM ANOVA), in spite of the progressive increases in HB/LG range LFP power and SNpr-MCx coherent oscillatory activity evident during the morning recording sessions (~18 h after 2nd D1+D2 antagonist injection) and deficits in the forepaw step test. These observations call attention to the disassociation between early expression of motor deficits and presence of beta range oscillatory activity after loss of dopamine receptor stimulation, highlighting the relatively slow, but consistent, increase in exaggerated levels of HB/LG LFP power and coherence, and the relatively rapid emergence, but less persistent expression of motor deficits.

3.7. Chronic dopamine receptor blockade in unilaterally lesioned rats: Days 0 & 6

A second approach to exploring whether increases in synchronized HB/LG range LFP activity could be observed after chronic D1+D2 antagonist treatment involved assessing the effects of administering D1+D2 antagonists twice daily to a group of rats which had

previously received unilateral injection of 6-OHDA (Fig. 4). The goal was to provide insight into whether HB/LG activity could be enhanced in motor circuits when a rat which had experienced chronic loss of dopamine receptor stimulation was in a cataleptic state, i.e. unable to initiate walking. These rats (n = 5) were unilaterally lesioned with 6-OHDA and allowed to recover for 7 days before initiation of twice-daily D1+D2 antagonist treatment for 7 additional days. SNpr-MCx electrode bundles were implanted in both lesioned and non-lesioned hemispheres at the time of the 6-OHDA lesion. LFP recordings from the MCx and SNpr were initiated a week after 6-OHDA lesion, 1 hour following the first D1+D2 antagonist treatment (Day 0) and 1 hour following the 7th D1+D2 antagonist treatment on Day 6 at a time when the animals were cataleptic. Rats were manually moved in the cylinder to approximate volitional motor behavior.

As shown by changes in the 6-OHDA lesioned hemisphere (Fig. 4D-F), investigator-assisted movement (see methods) did trigger a state associated with an increase in high beta activity in the lesioned hemisphere, even though the rat was incapable of moving on his own. This served to confirm that the investigator-assisted movement would be sufficient to induce increases in HB/LG activity in the non-lesioned hemisphere if beta-generating mechanisms have emerged in the non-lesioned hemisphere after chronic D1+D2 antagonist treatment.

Consistent with results from the D1+D2 antagonist-treated rats recorded after recovery from catalepsy (Fig. 3), these unilaterally lesioned rats receiving chronic DA antagonist treatment, with recordings performed while in a state of catalepsy, also showed in the non-lesioned hemisphere a progressive development of HB/LG synchronized activity in the MCx (Fig. 4A). Significant increases in MCx LFP power ($p = 0.014$, $F_{(2,8)} = 7.706$, n = 5, one way RM ANOVA) and MCx-SNpr coherence ($p < 0.001$, $F_{(2,8)} = 24.636$, n = 5, one way RM ANOVA) emerged in the non-lesioned hemisphere over the 7 days of chronic blockade of DA receptors (Fig. 4C, line graph and bar graph). Increases in both MCx LFP power and MCx-SNpr coherence became significant on Day 6 of treatment (MCx power: $p = 0.024$, $t = 3.220$; MCx-SNpr coherence: $p < 0.001$, $t = 5.910$, Holm-Sidak *post hoc*).

3.8. Acute effects of dopamine receptor blockade and dopamine transmission blockade

As shown in the preceding sections, rats display robust and persistent motor deficits on Day 1 while HB/LG power and/or coherence gradually increases over the 7 day period following either a unilateral 6-OHDA lesion (Fig. 1), bilateral 6-OHDA lesion (Fig. 2), or initiation of a chronic D1+D2 antagonist treatment regimen (Fig. 3). These results argue against a causal role for increases in HB/LG power alone in the induction of parkinsonian motor deficits and support the view that other processes may be responsible for the initial expression of motor symptoms. Specifically, as a significant shift in median peak frequency of mid-gamma LFP peaks occurred by Day 1, prior to significant increases in SNpr or MCx LFP total power in HB/LG frequency range in these 6-OHDA-lesioned rats, we were interested in a closer examination of LFP and motor activity in the earliest hours post-intervention. To explore this issue, MCx and SNpr LFP recordings were obtained within hours post-treatment from three groups of rats using 3 different approaches to acutely reduce dopamine-mediated neurotransmission.

The first group of rats (n = 6) received unilateral 6-OHDA infusions into the median forebrain bundle and LFPs were recorded from MCx and SNpr within 3–4 hours post infusion of 6-OHDA, at the earliest time point when the rats had recovered from the infusion procedure sufficiently to allow evaluation of their motor behavior. The second group of rats (n = 10 rats, 14 hemispheres) received D1+D2 antagonist injections with recordings performed over the 1–7 h period after antagonist administration (Fig. 5G-K) and the third group of rats (n = 3, 4 hemispheres) received microinfusions of tetrodotoxin (TTX) into the medial forebrain bundle (MFB) to block neurotransmission in the dopaminergic axons passing through this area. Recordings were performed 1–7 hours after TTX administration.

The rats in group 1, prior to 6-OHDA infusion into the MFB, had median peak frequencies in the MCx power spectra of 43.0 Hz (IQR: 41.3–46.9, n = 30). At 3–4 hours post-infusion the median peak frequency was significantly lower (36.1 Hz, $p < 0.001$, U = 135, n = 25, Mann-Whitney rank sum test), while total HB/LG power in MCx and SNpr and mean MCx-SNpr coherence were not different from control (Fig. 5A-C). Indeed, changes in the peak frequency of MCx power spectra emerged in conjunction with the emergence of severe unilateral motor deficit (Fig. 5D-F) as indicated by forelimb step test ($p = 0.012$, $F_{(1,2)} = 82.418$, n = 3 rats, two way RM ANOVA) and treadmill walking ($p = 0.012$, $F_{(1,5)} = 14.679$, n = 6 rats, two way RM ANOVA).

The second group of rats (n = 10 rats, 14 hemispheres), which received D1+D2 antagonist injections (Fig. 5G-K), showed a significant reduction in median peak frequency in the MCx observed within 1 hour after treatment (41.0 Hz vs. 33.2 Hz; $p < 0.001$, U = 668.5, n = 66 peaks in control and n = 45 peaks at 1 h post-treatment, Mann-Whitney rank sum test), along with a very modest but significant increase ($p = 0.04$, $F_{(4,40)} = 2.778$, n = 14, one way RM ANOVA) in MCx-SNpr coherence in HB/LG frequency range at 1 hour ($p = 0.024$, $t = 2.894$, Holm-Sidak *post hoc*). This reduction in peak frequency was accompanied by a marked decrease in motor activity, as the rats showed severe catalepsy (Fig. 5J-K), lasting for 6–7 h, as measured by the time spend on a grid and bar (Fig. 5K, grid: $p < 0.001$, $X^2 = 43.129$, df = 5, n = 10, RM ANOVA on ranks; Fig. 5K, bar: $p < 0.001$, $X^2 = 44.253$, df = 5, n = 10, RM ANOVA on Ranks) and also by the forelimb step_ test (Fig. 5J, left paw: $p < 0.001$, $X^2 = 37.333$, df = 4, n = 10, RM ANOVA on Ranks; right paw: $p < 0.001$, $X^2 = 33.528$, df = 4, n = 10, RM ANOVA on Ranks).

The third group of rats, which received unilateral infusion of TTX into the MFB, developed long-lasting (~5 h) unilateral deficits in the forelimb stepping test (Fig. 5O) immediately after TTX microinjection ($p < 0.001$, $F_{(4,12)} = 70.229$, one way RM ANOVA). The paw contralateral to the infusion (grey bars) exhibited step counts significantly lower than control at hours 1, 2, and 3 post-infusion ($p < 0.001$, Holm-Sidak *post hoc*). At the same time, the paw ipsilateral to the infusion (green bars) did not show a decrease in step counts post-TTX administration ($p = 0.704$, $F_{(4,12)} = 0.549$, one way RM ANOVA). Similar to rats with unilateral 6-OHDA lesion, these animals exhibited difficulty walking in the circular treadmill in the direction contralateral to the infusion, immediately after TTX administration (Fig. 5P, grey bars; $p = 0.004$, $F_{(4,12)} = 7.097$, one way RM ANOVA), but retained the ability to walk ipsilaterally (purple bars, $p = 0.292$, $F_{(4,12)} = 1.399$, one way RM ANOVA). The TTX-induced motor dysfunction in contralateral walking was significant at hours one

($p < 0.05$, $t = 4.352$) and two ($p < 0.05$, $t = 2.915$, Holm-Sidak post hoc) and gradually improved over the course of 3–7 hours, reaching a level similar to control at hour 5 ($p = 0.911$, $t = 0.389$, Holm-Sidak *post hoc*). Rats did not show motor deficits 24 hours after the administration of TTX into the MFB ($p = 0.979$, $t = 0.027$, Holm-Sidak *post hoc*).

In conjunction with the severe TTX-induced impairment of motor function, a significant decrease in median peak frequency was observed in the MCx LFP spectra (Fig. 5L, bar graph, inset) at one hour post-TTX infusion (median: 39.6 Hz at 1 hour, n = 12 peaks vs. 42.0 Hz in control, n = 17 peaks, $p = 0.014$, $U = 46.5$, Mann-Whitney Rank Sum). As displayed in the LFP recordings, SNpr did not show dominant peaks in power spectra in the HB/LG range over this time periods. Instead, modest decreases in SNpr LFP power were observed in a broad range of frequencies, 29 – 55 Hz (Fig. 5M). at 1 and 3 hours (high beta: $p = 0.003$ and $p = 0.046$, respectively) with full recovery to control level by ~5 hours (data not shown).

Overall, the results indicate that an acute interruption of dopamine transmission with TTX infusion into the MFB does not result in the emergence of coherent beta-range oscillatory activity in the SNpr–MCx circuitry (Fig. 5N), although it does rapidly induce significant and long-lasting motor deficits.

This examination shows that three interventions designed to interrupt normal dopamine receptor stimulation in the behaving rat induce an early shift in the peak frequency of cortical mid-gamma activity on a time scale similar to the emergence of parkinsonian motor deficits. This contrasts with the more gradual increases in total HB/LG power and mean coherence that emerge in the MCx-SNpr circuit in the days after either dopamine cell lesion or commencement of chronic D1+D2 antagonist treatment, which are not associated with further progression in motor dysfunction.

3.6. Apomorphine administration after unilateral 6-OHDA-induced dopamine cell lesion: Day 1–2

To gain further insight into the relationship between the shift in peak frequencies as a correlate of early changes in motor function after DA cell lesion, a separate group of rats (n = 6) were treated with low dose (0.075–0.1 mg/kg, s.c.) of apomorphine, a non-specific dopamine receptor agonist, on Day 1 and Day 2 following unilateral 6-OHDA-induced DA cell lesion. As shown in Fig. 6A and Fig. 6C, significant increases in HB/LG MCx LFP power ($p = 0.014$, $F_{(4,20)} = 4.089$, n = 6 rats, one way RM ANOVA) and MCx-SNpr coherence ($p < 0.001$, $F_{(4,20)} = 20.826$, n = 6 rats, one way RM ANOVA) emerged on Days 1 (MCx: $p = 0.017$, $t = 2.909$; MCx-SNpr: $p < 0.001$, $t = 4.482$, Holm-Sidak *post hoc*) and Day 2 (MCx: $p = 0.009$, $t = 3.502$; MCx-SNpr: $p < 0.001$, $t = 7.772$, Holm-Sidak *post hoc*) after infusion of neurotoxin 6-OHDA relative to control.

Stimulation of DA receptors with apomorphine on Day 1 and Day 2 post-lesion led to large reduction in mean HB/LG range MCx-SNpr coherence, resulting in values similar to control (Fig. 6C, light grey bars, Day 1: $p = 0.446$, $t = 1.170$; Day 2: $p = 0.381$, $t = 0.896$, Holm-Sidak *post hoc*). A similar reduction in HB/LG SNpr LFP power and MCx-SNpr coherence spectra emerged after apomorphine treatment (Fig. 6B, C, insets). These results

are similar to changes observed in power and coherence in MCx and STN in early studies in awake behaving rats 4 – 5 weeks post lesion (Sharott et al., 2005). Interestingly, in the present study, while apomorphine reduced the high beta/low gamma LFP power in the MCx, it also significantly increased MCx LFP total power in the gamma frequency range relative to control ($p = 0.001$, $X^2 = 17.733$, RM ANOVA on Ranks) on post-lesion Day 1 ($p < 0.05$, $Q = 2.739$) and Day 2 ($p < 0.05$, $Q = 2.556$, Dunn's *post hoc*) as indicated by plus signs in the MCx bar graph, Fig. 6A.

Results in Fig. 6D also show the ability of apomorphine to largely reverse the decrease in peak frequency induced by the dopamine cell lesion. 6-OHDA lesion-induced a reduction ($p < 0.05$, $H = 36.069$, $df = 4$, ANOVA on Ranks) in median peak frequency in the MCx LFP in the 29–55 Hz range from control (44.4 Hz, n = 30) to 37.1 Hz on Day 1 post-lesion ($p < 0.05$, $Q = 3.234$, n = 29, Dunn's post hoc) and to 32.2 Hz on Day 2 post-lesion ($p < 0.05$, $Q = 5.375$, n = 18, Dunn's post hoc). Administration of apomorphine induced shifts in the median peak frequency (Fig. 6D) in the MCx power from the HB/LG range on post-lesion Day 1 and Day 2 (medians: 37.1 and 32.2 Hz, respectively) to values statistically similar to control (44.4 Hz) in the gamma frequency range (medians: 43.0 Hz, n = 24 and 40.5 Hz, n = 28 on Day 1 + Apo and Day 2 + Apo, respectively; $p > 0.05$, $Q = 2.070$, $Q = 0.508$, ANOVA on Ranks).

Concurrent with reduction of SNpr LFP power and MCx-SNpr coherence and marked increases in cortical spectral peak frequency from HB/LG to the mid-gamma range, significant improvements in contralateral treadmill walking were observed from 10 to 40 min after the administration of apomorphine ($p < 0.001$, $F_{(4, 20)} = 25.167$, n = 6 rats, one way RM ANOVA) on Day 1 ($p < 0.001$, $t = 5.236$) and Day 2 ($p < 0.001$, $t = 6.724$, Holm-Sidak *post hoc*) evidenced from the increases in the in/out step ratios (Fig. 6E) and percentage of completed trials in the contralateral walking on a circular treadmill (Fig. 6F).

Similar to results seen in the hours following reduction of dopamine receptor stimulation (Fig. 5), the administration of apomorphine to rats with unilateral 6-OHDA lesion provides evidence that shifts in the peak frequency of HB/LG and mid-gamma MCx LFP activity brought on by manipulation of dopamine function occur on a timescale similar to concomitant alterations of motor behavior. Namely, when dopamine receptor stimulation is attenuated (either through 6-OHDA cell lesion, administration of dopamine cell antagonists, or interruption of dopaminergic transmission by TTX), motor deficits emerge on a similar timescale as the downward shift of the peak frequency in MCx LFP power spectra from mid-gamma to HB/LG range. When dopamine function is partially restored through the administration of a dopamine cell agonist, motor function recovers and LFP power in the mid-gamma range around 41–55 Hz is subsequently restored.

4. Discussion

The present investigation sought to gain insight into the relationship between increased beta range LFP activity and the emergence of motor symptoms in parkinsonian rats through a detailed assessment of changes in MCx and SNpr LFP activity over the first hours and days following application of different strategies for interruption of dopamine receptor

stimulation. This study was motivated by previous results in our lab which showed that high beta LFP activity in the parkinsonian rat basal ganglia exhibits amplitude modulation during treadmill walking in conjunction with the rat's stepping cycle (Brazhnik et al., 2014; Delaville et al., 2015), a pattern resembling the desynchronization, followed by resynchronization of beta oscillations observed in the STN in PD patients during ongoing movements (Kuhn et al., 2004; Doyle et al., 2005; Joundi et al., 2013; Heinrichs-Graham et al., 2017). In view of this degree of face validity, it was hypothesized that rat models for PD could provide further insight into whether the exaggerated beta range activity plays a causal role in the early emergence of motor symptoms in PD patients.

Initial focus was on the early effects of 6-OHDA unilateral and bilateral dopamine cell lesion. The circular treadmill walking task facilitated consistent quantification and accommodation of the presence of bradykinesia in conjunction with the neurophysiological recordings over this time period. (Avila et al., 2010; Brazhnik et al., 2012; Brazhnik et al., 2014). Results showed motor symptoms emerging before significant increases in beta range LFP power were evident in the motor cortex or basal ganglia. These observations are inconsistent with the idea that exaggerated beta range activity, as measured by averaged LFP power, plays a causal role in inducing motor symptoms. They are, however, consistent with other evidence that motor symptoms precede development of exaggerated synchronization of activity in beta range in the basal ganglia, as shown by spiking data from the GPi in MPTP-lesioned primates (Leblois et al., 2007) as well as ECoG and LFP recordings from MCx (Mallet et al., 2008; Degos et al., 2009) in 6-OHDA lesioned rats and LFP recordings from the SNpr in partially lesioned rats (Quiroga-Varela et al., 2013).

Our second strategy for assessing early changes in a rat model for PD involved twice daily treatments for a week with D1+D2 dopamine receptor antagonists. The lack of evidence linking increases in beta range activity with catalepsy induced by acute administration of dopamine receptor antagonists has also raised doubts about a causal relationship between exaggerated beta range activity and motor dysfunction (Degos et al., 2009). The present results further support the view that emergence of exaggerated beta range activity requires loss of dopamine receptor stimulation over a longer time frame than necessary for the expression of profound motor deficits. Moreover, once established, exaggerated LFP activity remains evident during treadmill walking for several days after catalepsy has worn off.

The more rapid emergence of motor symptoms, relative to changes in HB/LG LFP power in these parkinsonian models, prompted a closer look at data from the first hours post-treatment. Included in this examination was a third model for PD: rats treated acutely with injections of TTX into the MFB to block impulse flow in the dopaminergic axons in this bundle (Galati et al., 2009). All three models showed a rapid loss of the significant, relatively broad peak in MCx LFP power normally evident during treadmill walking in the mid-gamma range, around 43 Hz. This early decrease in MCx LFP activity in the 41 – 45 Hz range appears tightly correlated with the emergence of the motor symptoms in these parkinsonian models, in contrast to the more gradual increase in the beta range associated with these motor deficits. The loss of this mid-gamma oscillatory activity was also readily reversed in the lesioned rats, along with improvement in contralateral treadmill walking, by administration of apomorphine, a dopamine agonist on day 1 or day 2 post-lesion. An

additional early change observed following dopamine cell lesion or antagonist treatment was a gradual increase in coherence between MCx and SNpr LFPs in the 29– 40 Hz range, significant by day 1 after the 6-OHDA infusion, and by hour 1 after D1+D2 antagonist administration.

Thus, the picture that emerges following loss of dopamine receptor simulation is one of a rapid loss of cortical LFP synchronization in the mid-gamma range in conjunction with a concomitant appearance of motor deficits. This is followed by gradually increasing spike-LFP coherence between motor cortex activity and basal ganglia output in the HB/LG ranges, and emergence, over subsequent days, of significant increases in oscillatory activity and LFP power in the high beta range. It should be noted that while mean multiunit SNpr spike rates were not increased over time post lesion relative to controls, this result cannot be taken to indicate that single unit SNpr firing rates were unaltered in this PD model as the number of units participating in the multi-unit spike trains could be variable. Our novel observation of an early decrease in MCx activity the mid-gamma Hz range in conjunction with the emergence of motor deficits in treadmill walking in the parkinsonian rat is intriguing in light of recent reports that increases in gamma range activity in M1 cortex in healthy humans during treadmill walking are associated with high-level motor control of gait (McCrimmon et al., 2018; Delval et al., 2020). Also relevant may be the recent report that enhancing gamma oscillations via transcranial alternating current stimulation restores primary motor cortex plasticity in Parkinson’s disease patients (Guerra et al., 2020). An interesting question is whether the early change in MCx function reflects a direct effect of decreased dopamine receptor stimulation on MCx circuitry, or an indirect effect, i.e. a change in input to the motor cortex, triggered by changes in the striatum or thalamus or other areas affected by loss of dopamine (Arbuthnott and Garcia-Munoz, 2017; Vitrac and Benoit-Marand, 2017; Hyland et al., 2019; Mallet et al., 2019; Cousineau et al., 2020). Related to this is the increase by day 1 in coherence between SNpr LFP and MCx in the HB/LG range. This argues that however the early decrease in the MCx mid-gamma range MCx frequency is triggered, downstream activity patterns are also impacted before the significant build-up of beta range power emerges. While it remains to be seen how this coherence is established, the increase in MCx-SNpr coherence may be a marker of early functional disruption in basal ganglia output. It seems probable that the subsequent more gradual build-up of exaggerated beta range power in the basal ganglia circuits over time after loss of dopamine receptor stimulation is entrained by the substantial plasticity-induced changes in synaptic and circuit function in the basal ganglia-thalamocortical network which have been described in a number of studies in rodent and primate PD models (Villalba and Smith, 2018; Kovaleski et al., 2020).

While it has been difficult to conclude from studies in PD patients whether the exaggerated beta rhythms in the STN and MCx play a causal, epiphenomenal or maladaptive role with respect to motor symptoms (Neumann et al., 2016; Geng et al., 2018; Singh, 2018; Wichmann et al., 2018; Schmidt et al., 2020), the current results join a handful of studies in animal models (Leblois et al., 2007; Mallet et al., 2008; Degos et al., 2009; Quiroga-Varela et al., 2013) arguing that this activity is not directly causal of the motor symptoms. The extent to which the exaggerated beta activity is, instead, compensatory, epiphenomenal or maladaptive in PD patients remains a matter of on-going interest, however, as clinical

studies fine-tune the use of beta range activity to trigger closed-loop feedback and phase-dependent stimulation paradigms for enhancing the efficacy of DBS in PD patients (Tinkhauser et al., 2017; Little and Brown, 2020).

In this context it is important to point out two caveats with respect to the implications of the current study. First, it should be noted that the current data is derived from LFP power in a narrow band surrounding the peak frequency, averaged over 60 second walking epochs. Future investigations should determine whether more subtle changes in amplitude, timing, duration or incidence of discrete beta bursts might be more causally correlated with early motor deficits. Evidence from PD patients supports the idea that the cumulative number and timing of individual beta bursts, as opposed to mean power, might be more predictive of a delay in movement initiation, leaving open the potential for further debate about causation (Torrecillos et al., 2018; Tinkhauser et al., 2020).

A second important caveat has to do with the more general issue of the translatability of pathophysiological observations in rodent models for PD to PD patients. In particular, it's been noted that the frequency ranges of exaggerated LFP beta activity associated with motor deficits vary across species (Stein and Bar-Gad, 2013; Galvan et al., 2015; Smith and Galvan, 2018; Whalen et al., 2020). The mechanisms responsible for this variability remain unclear, as do the implications for the validity of animal models for PD. As shown in the current study, LFP activity in the 30–35 Hz range is strikingly prominent in the awake behaving parkinsonian rats (Avila et al., 2010; Brazhnik et al., 2014; Delaville et al., 2015; Brazhnik et al., 2016; Dupre et al., 2016), and represents a higher frequency than the exaggerated 13–30 Hz beta range activity more typically reported in recordings from human patients. Non-human primates models of PD also have excessive beta but the peak frequencies are typically described in the low beta range (Stein and Bar-Gad, 2013; Galvan et al., 2015; Smith and Galvan, 2018; Deffains and Bergman, 2019). Mice show increased LFP activity in delta ranges when active and are not reported to have exaggerated beta range activity (Schor and Nelson, 2019; Willard et al., 2019; Whalen et al., 2020).

Relevant to these considerations, however, is clear evidence that the peak frequency of exaggerated LFP activity in basal ganglia-thalamocortical circuits in dopamine cell lesioned rats is highly behavioral state dependent (Walters et al., 2007; Mallet et al., 2008; Avila et al., 2010; Brazhnik et al., 2012; Brazhnik et al., 2014). Clinical studies have also found LFP peak frequencies in the 12 – 35 Hz beta range recorded in motor cortex and STN vary across patients but are typically consistent within a given setting for an individual patient (Kuhn et al., 2008). These considerations argue for the benefit of determining most relevant peak frequency range in individual animal models or patients when using beta range power as a biomarker for DBS or an indication of the success of an intervention or treatment.

4.1. Conclusion

In summary, these data do not support a role for beta range activity as being causal of bradykinesia in the early hours post-lesion or following chronic dopamine antagonist treatment. However, they are consistent with the potential of this signal as a biomarker reflecting the impact of loss of dopamine on basal ganglia circuit function, reliably induced by loss of dopamine yet rapidly attenuated by dopamine replacement therapy or DBS.

Thus, they are promising as a trigger for closed-loop feedback of DBS. Moreover, novel observations from the early hours and days following reduction of dopamine receptor stimulation in three different models of PD call attention to the potential significance of the early decrease in mid-gamma range activity in the MCx with respect to the emergence of motor symptoms. Further understanding of the role of dopaminergic transmission in the maintenance of ongoing activity in the motor cortex during treadmill walking may provide insight into additional strategies for reduction of bradykinesia.

Supplementary Material

Refer to Web version on PubMed Central for supplementary material.

Acknowledgements:

The Intramural Research Program of the NINDS, NIH supported this research. We wish to thank Newlin, Morgan, Tom Talbot and Daryl Brandy in the Research Services Branch for design and fabrication of the rotary treadmill.

Funding: The Intramural Research Program of the NIHDS, NIH supported this research.

Abbreviations:

6-OHDA	6-hydroxydopamine HBr
Apo	apomorphine
BG	basal ganglia
DA	dopamine
DBS	deep brain stimulation
HB/LG	high beta/low gamma
IQR	interquartile range
L-dopa	levodopa
LFP	local field potential
MCx	motor cortex
MFB	medial forebrain bundle
PL	post-lesion
PD	Parkinso’s disease
RPM	rotations per minute
SNpr	substantia nigra pars reticulata
STN	subthalamic nucleus
STWA	spike-triggered LFP waveform average

TTX tetrodotoxin

References

Ahlenius S, Hillegaart VD (1986) Involvement of extrapyramidal motor mechanisms in the suppression of locomotor activity by antipsychotic drugs: A comparison between the effects produced by pre- and post-synaptic inhibition of dopaminergic neurotransmission. Pharmacol Biochem Behav 24:1409–1415. [PubMed: 2873588]

Alonso-Frech F, Zamarbide I, Alegre M, Rodriguez-Oroz MC, Guridi J, Manrique M, Valencia M, Artieda J, Obeso JA (2006) Slow oscillatory activity and levodopa-induced dyskinesias in parkinson's disease. Brain 129:1748–1757. [PubMed: 16684788]

Arbuthnott GW, Garcia-Munoz M (2017) Are the symptoms of parkinsonism cortical in origin? Comput Struct Biotechnol J 15:21–25. [PubMed: 28694933]

Avila I, Parr-Brownlie LC, Brazhnik E, Castaneda E, Bergstrom DA, Walters JR (2010) Beta frequency synchronization in basal ganglia output during rest and walk in a hemiparkinsonian rat. Exp Neurol 221:307–319. [PubMed: 19948166]

Brazhnik E, Novikov N, McCoy AJ, Cruz AV, Walters JR (2014) Functional correlates of exaggerated oscillatory activity in basal ganglia output in hemiparkinsonian rats. Exp Neurol 261:563–577. [PubMed: 25084518]

Brazhnik E, McCoy AJ, Novikov N, Hatch CE, Walters JR (2016) Ventral medial thalamic nucleus promotes synchronization of increased high beta oscillatory activity in the basal ganglia-thalamocortical network of the hemiparkinsonian rat. J Neurosci 36:4196–4208. [PubMed: 27076419]

Brazhnik E, Cruz AV, Avila I, Wahba MI, Novikov N, Ilieva NM, McCoy AJ, Gerber C, Walters JR (2012) State-dependent spike and local field synchronization between motor cortex and substantia nigra in hemiparkinsonian rats. J Neurosci 32:7869–7880. [PubMed: 22674263]

Brittain JS, Brown P (2014) Oscillations and the basal ganglia: Motor control and beyond. Neuroimage 85 Pt 2:637–647.

Brown P (2003) Oscillatory nature of human basal ganglia activity: Relationship to the pathophysiology of parkinson's disease. Mov Disord 18:357–363. [PubMed: 12671940]

Brown P, Oliviero A, Mazzone P, Insola A, Tonali P, Di Lazzaro V (2001) Dopamine dependency of oscillations between subthalamic nucleus and pallidum in parkinson's disease. J Neurosci 21:1033–1038. [PubMed: 11157088]

Cassidy M, Mazzone P, Oliviero A, Insola A, Tonali P, Di Lazzaro V, Brown P (2002) Movement-related changes in synchronization in the human basal ganglia. Brain 125:1235–1246. [PubMed: 12023312]

Cousineau J, Lescouzeres L, Taupignon A, Delgado-Zabalza L, Valjent E, Baufreton J, Le Bon-Jego M (2020) Dopamine d2-like receptors modulate intrinsic properties and synaptic transmission of parvalbumin interneurons in the mouse primary motor cortex. eNeuro 7.

Cruz AV, Mallet N, Magill PJ, Brown P, Averbeck BD (2009) Effects of dopamine depletion on network entropy in the external globus pallidus. J Neurophysiol 102:1092–1102. [PubMed: 19535481]

Deffains M, Bergman H (2019) Parkinsonism-related beta oscillations in the primate basal ganglia networks - recent advances and clinical implications. Parkinsonism & related disorders 59:2–8. [PubMed: 30578010]

Degos B, Deniau JM, Chavez M, Maurice N (2009) Chronic but not acute dopaminergic transmission interruption promotes a progressive increase in cortical beta frequency synchronization: Relationships to vigilance state and akinesia. Cereb Cortex 19:1616–1630. [PubMed: 18996909]

Dejean C, Gross CE, Bioulac B, Boraud T (2008) Dynamic changes in the cortex-basal ganglia network after dopamine depletion in the rat. Journal of Neurophysiology 100:385–396. [PubMed: 18497362]

Delaville C, McCoy AJ, Gerber CM, Cruz AV, Walters JR (2015) Subthalamic nucleus activity in the awake hemiparkinsonian rat: Relationships with motor and cognitive networks. J Neurosci 35:6918–6930. [PubMed: 25926466]

Delaville C, Cruz AV, McCoy AJ, Brazhnik E, Avila I, Novikov N, Walters JR (2014) Oscillatory activity in basal ganglia and motor cortex in an awake behaving rodent model of parkinson's disease. Basal Ganglia 3:221–227. [PubMed: 25667820]

Delval A, Bayot M, Defebvre L, Dujardin K (2020) Cortical oscillations during gait: Wouldn't walking be so automatic? Brain Sci 10.

Dostrovsky J, Bergman H, Hutchison WD, Dostrovsky JO, Walters JR, Courtemanche R, Boraud T, Goldberg J, Brown P (2004) Oscillatory activity in the basal ganglia--relationship to normal physiology and pathophysiology. Brain 127:721–722. [PubMed: 15044311]

Doyle LM, Kuhn AA, Hariz M, Kupsch A, Schneider GH, Brown P (2005) Levodopa-induced modulation of subthalamic beta oscillations during self-paced movements in patients with parkinson's disease. Eur J Neurosci 21:1403–1412. [PubMed: 15813950]

Dupre KB, Cruz AV, McCoy AJ, Delaville C, Gerber CM, Eyring KW, Walters JR (2016) Effects of ldopa priming on cortical high beta and high gamma oscillatory activity in a rodent model of parkinson's disease. Neurobiol Dis 86:1–15. [PubMed: 26586558]

Ellens DJ, Leventhal DK (2013) Review: Electrophysiology of basal ganglia and cortex in models of parkinson disease. Journal of Parkinson's disease 3:241–254.

Fischer P, Chen CC, Chang YJ, Yeh CH, Pogosyan A, Herz DM, Cheeran B, Green AL, Aziz TZ, Hyam J, Little S, Foltynie T, Limousin P, Zrinzo L, Hasegawa H, Samuel M, Ashkan K, Brown P, Tan H (2018) Alternating modulation of subthalamic nucleus beta oscillations during stepping. J Neurosci 38:5111–5121. [PubMed: 29760182]

Galati S, Stanzione P, D'Angelo V, Fedele E, Marzetti F, Sancesario G, Procopio T, Stefani A (2009) The pharmacological blockade of medial forebrain bundle induces an acute pathological synchronization of the cortico-subthalamic nucleus-globus pallidus pathway. J Physiol 587:4405–4423. [PubMed: 19622605]

Galvan A, Devergnas A, Wichmann T (2015) Alterations in neuronal activity in basal ganglia-thalamocortical circuits in the parkinsonian state. Front Neuroanat 9:5. [PubMed: 25698937]

Geng X, Xu X, Horn A, Li N, Ling Z, Brown P, Wang S (2018) Intra-operative characterisation of subthalamic oscillations in parkinson's disease. Clin Neurophysiol 129:1001–1010. [PubMed: 29567582]

Giannicola G, Marceglia S, Rossi L, Mrakic-Sposta S, Rampini P, Tamma F, Cogiamanian F, Barbieri S, Priori A (2010) The effects of levodopa and ongoing deep brain stimulation on subthalamic beta oscillations in parkinson's disease. Exp Neurol 226:120–127. [PubMed: 20713047]

Guerra A, Asci F, D'Onofrio V, Sveva V, Bologna M, Fabbrini G, Berardelli A, Suppa A (2020) Enhancing gamma oscillations restores primary motor cortex plasticity in parkinson's disease. J Neurosci 40:4788–4796. [PubMed: 32430296]

Heinrichs-Graham E, Santamaria PM, Gendelman HE, Wilson TW (2017) The cortical signature of symptom laterality in parkinson's disease. Neuroimage Clin 14:433–440. [PubMed: 28271041]

Hell F, Plate A, Mehrkens JH, Botzel K (2018) Subthalamic oscillatory activity and connectivity during gait in parkinson's disease. Neuroimage Clin 19:396–405. [PubMed: 30035024]

Hell F, Palleis C, Mehrkens JH, Koeglsperger T, Botzel K (2019) Deep brain stimulation programming 2.0: Future perspectives for target identification and adaptive closed loop stimulation. Front Neurol 10:314. [PubMed: 31001196]

Hoffman DC, Donovan H (1995) Catalepsy as a rodent model for detecting antipsychotic drugs with extrapyramidal side effect liability. Psychopharmacology (Berl) 120:128–133. [PubMed: 7480543]

Hutchison WD, Dostrovsky JO, Walters JR, Courtemanche R, Boraud T, Goldberg J, Brown P (2004) Neuronal oscillations in the basal ganglia and movement disorders: Evidence from whole animal and human recordings. J Neurosci 24:9240–9243. [PubMed: 15496658]

Hyland BI, Seeger-Armbruster S, Smither RA, Parr-Brownlie LC (2019) Altered recruitment of motor cortex neuronal activity during the grasping phase of skilled reaching in a chronic rat model of unilateral parkinsonism. J Neurosci 39:9660–9672. [PubMed: 31641050]

Javor-Duray BN, Vinck M, van der Roest M, Mulder AB, Stam CJ, Berendse HW, Voorn P (2015) Early-onset cortico-cortical synchronization in the hemiparkinsonian rat model. Journal of neurophysiology 113:925–936. [PubMed: 25392174]

Joundi RA, Brittain JS, Green AL, Aziz TZ, Brown P, Jenkinson N (2013) Persistent suppression of subthalamic beta-band activity during rhythmic finger tapping in parkinson's disease. Clin Neurophysiol 124:565–573. [PubMed: 23085388]

Kovaleski RF, Callahan JW, Chazalon M, Wokosin DL, Baufreton J, Bevan MD (2020) Dysregulation of external globus pallidus-subthalamic nucleus network dynamics in parkinsonian mice during cortical slow-wave activity and activation. J Physiol 598:1897–1927. [PubMed: 32112413]

Kuhn AA, Kupsch A, Schneider GH, Brown P (2006) Reduction in subthalamic 8–35 hz oscillatory activity correlates with clinical improvement in parkinson's disease. Eur J Neurosci 23:1956–1960. [PubMed: 16623853]

Kuhn AA, Williams D, Kupsch A, Limousin P, Hariz M, Schneider GH, Yarrow K, Brown P (2004) Event-related beta desynchronization in human subthalamic nucleus correlates with motor performance. Brain 127:735–746. [PubMed: 14960502]

Kuhn AA, Tsui A, Aziz T, Ray N, Brucke C, Kupsch A, Schneider GH, Brown P (2008) Pathological synchronisation in the subthalamic nucleus of patients with parkinson's disease relates to both bradykinesia and rigidity. Exp Neurol 215:380–387. [PubMed: 19070616]

Leblois A, Meissner W, Bioulac B, Gross CE, Hansel D, Boraud T (2007) Late emergence of synchronized oscillatory activity in the pallidum during progressive parkinsonism. Eur J Neurosci 26:1701–1713. [PubMed: 17880401]

Levy R, Hutchison WD, Lozano AM, Dostrovsky JO (2000) High-frequency synchronization of neuronal activity in the subthalamic nucleus of parkinsonian patients with limb tremor. J Neurosci 20:7766–7775. [PubMed: 11027240]

Levy R, Ashby P, Hutchison WD, Lang AE, Lozano AM, Dostrovsky JO (2002) Dependence of subthalamic nucleus oscillations on movement and dopamine in parkinson's disease. Brain 125:1196–1209. [PubMed: 12023310]

Little S, Brown P (2020) Debugging adaptive deep brain stimulation for parkinson's disease. Mov Disord 35:555–561. [PubMed: 32039501]

Lofredi R, Tan H, Neumann WJ, Yeh CH, Schneider GH, Kuhn AA, Brown P (2019) Beta bursts during continuous movements accompany the velocity decrement in parkinson's disease patients. Neurobiol Dis 127:462–471. [PubMed: 30898668]

Mallet N, Delgado L, Chazalon M, Miguelez C, Baufreton J (2019) Cellular and synaptic dysfunctions in parkinson's disease: Stepping out of the striatum. Cells 8.

Mallet N, Pogosyan A, Sharott A, Csicsvari J, Bolam JP, Brown P, Magill PJ (2008) Disrupted dopamine transmission and the emergence of exaggerated beta oscillations in subthalamic nucleus and cerebral cortex. J Neurosci 28:4795–4806. [PubMed: 18448656]

Marsden JF, Limousin-Dowsey P, Ashby P, Pollak P, Brown P (2001) Subthalamic nucleus, sensorimotor cortex and muscle interrelationships in parkinson's disease. Brain 124:378–388. [PubMed: 11157565]

McCrimmon CM, Wang PT, Heydari P, Nguyen A, Shaw SJ, Gong H, Chui LA, Liu CY, Nenadic Z, Do AH (2018) Electrocorticographic encoding of human gait in the leg primary motor cortex. Cereb Cortex 28:2752–2762. [PubMed: 28981644]

Mirelman A, Bonato P, Camicioli R, Ellis TD, Giladi N, Hamilton JL, Hass CJ, Hausdorff JM, Pelosin E, Almeida QJ (2019) Gait impairments in parkinson's disease. Lancet Neurol 18:697–708. [PubMed: 30975519]

Molinet-Dronda F, Gago B, Quiroga-Varela A, Juri C, Collantes M, Delgado M, Prieto E, Ecay M, Iglesias E, Marin C, Penuelas I, Obeso JA (2015) Monoaminergic pet imaging and histopathological correlation in unilateral and bilateral 6-hydroxydopamine lesioned rat models of parkinson's disease: A longitudinal in-vivo study. Neurobiol Dis 77:165–172. [PubMed: 25681534]

Morelli M, Di Chiara GD (1985) Catalepsy induced by sch 23390 in rats. Eur J Pharmacol 117:179–185. [PubMed: 2866970]

Neumann WJ, Degen K, Schneider GH, Brucke C, Huebl J, Brown P, Kuhn AA (2016) Subthalamic synchronized oscillatory activity correlates with motor impairment in patients with parkinson's disease. Mov Disord 31:1748–1751. [PubMed: 27548068]

Nevado-Holgado AJ, Mallet N, Magill PJ, Bogacz R (2014) Effective connectivity of the subthalamic nucleus-globus pallidus network during parkinsonian oscillations. The Journal of physiology 592:1429–1455. [PubMed: 24344162]

Olsson M, Nikkhah G, Bentlage C, Bjorklund A (1995) Forelimb akinesia in the rat parkinson model: Differential effects of dopamine agonists and nigral transplants as assessed by a new stepping test. J Neurosci 15:3863–3875. [PubMed: 7751951]

Oswal A, Beudel M, Zrinzo L, Limousin P, Hariz M, Foltynie T, Litvak V, Brown P (2016) Deep brain stimulation modulates synchrony within spatially and spectrally distinct resting state networks in parkinson's disease. Brain 139:1482–1496. [PubMed: 27017189]

Park H, Youm C, Lee M, Noh B, Cheon SM (2020) Turning characteristics of the more-affected side in parkinson's disease patients with freezing of gait. Sensors (Basel) 20.

Pfurtscheller G, Stancak A Jr., Neuper C (1996) Post-movement beta synchronization. A correlate of an idling motor area? Electroencephalogr Clin Neurophysiol 98:281–293. [PubMed: 8641150]

Priori A, Foffani G, Pesenti A, Tamma F, Bianchi AM, Pellegrini M, Locatelli M, Moxon KA, Villani RM (2004) Rhythm-specific pharmacological modulation of subthalamic activity in parkinson's disease. Exp Neurol 189:369–379. [PubMed: 15380487]

Quinn EJ, Blumenfeld Z, Velisar A, Koop MM, Shreve LA, Trager MH, Hill BC, Kilbane C, Henderson JM, Bronte-Stewart H (2015) Beta oscillations in freely moving parkinson's subjects are attenuated during deep brain stimulation. Mov Disord 30:1750–1758. [PubMed: 26360123]

Quiroga-Varela A, Walters JR, Brazhnik E, Marin C, Obeso JA (2013) What basal ganglia changes underlie the parkinsonian state? The significance of neuronal oscillatory activity. Neurobiol Dis 58:242–248. [PubMed: 23727447]

Rodriguez M, Barroso-Chinea P, Abdala P, Obeso J, Gonzalez-Hernandez T (2001) Dopamine cell degeneration induced by intraventricular administration of 6-hydroxydopamine in the rat: Similarities with cell loss in parkinson's disease. Experimental neurology 169:163–181. [PubMed: 11312569]

Rosenberg JR, Amjad AM, Breeze P, Brillinger DR, Halliday DM (1989) The fourier approach to the identification of functional coupling between neuronal spike trains. Prog Biophys Mol Biol 53:131.

Schmidt SL, Peters JJ, Turner DA, Grill WM (2020) Continuous deep brain stimulation of the subthalamic nucleus may not modulate beta bursts in patients with parkinson's disease. Brain Stimul 13:433–443. [PubMed: 31884188]

Schor JS, Nelson AB (2019) Multiple stimulation parameters influence efficacy of deep brain stimulation in parkinsonian mice. J Clin Invest 129:3833–3838. [PubMed: 31194696]

Sharott A, Magill PJ, Harnack D, Kupsch A, Meissner W, Brown P (2005) Dopamine depletion increases the power and coherence of beta-oscillations in the cerebral cortex and subthalamic nucleus of the awake rat. Eur J Neurosci 21:1413–1422. [PubMed: 15813951]

Singh A (2018) Oscillatory activity in the cortico-basal ganglia-thalamic neural circuits in parkinson's disease. Eur J Neurosci 48:2869–2878. [PubMed: 29381817]

Smith Y, Galvan A (2018) Non-human primate research of basal ganglia and movement disorders: Advances and challenges. J Neural Transm (Vienna) 125:275–278. [PubMed: 29423879]

Sochurkova D, Rektor I (2003) Event-related desynchronization/synchronization in the putamen. An seeg case study. Exp Brain Res 149:401–404. [PubMed: 12632243]

Stein E, Bar-Gad I (2013) Beta oscillations in the cortico-basal ganglia loop during parkinsonism. Exp Neurol 245:52–59. [PubMed: 22921537]

Swan CB, Schulte DJ, Brocker DT, Grill WM (2019) Beta frequency oscillations in the subthalamic nucleus are not sufficient for the development of symptoms of parkinsonian bradykinesia/akinesia in rats. eNeuro 6.

Tinkhauser G, Pogosyan A, Little S, Beudel M, Herz DM, Tan H, Brown P (2017) The modulatory effect of adaptive deep brain stimulation on beta bursts in parkinson's disease. Brain : a journal of neurology 140:1053–1067. [PubMed: 28334851]

Tinkhauser G, Torrecillos F, Pogosyan A, Mostofi A, Bange M, Fischer P, Tan H, Hasegawa H, Glaser M, Muthuraman M, Groppa S, Ashkan K, Pereira EA, Brown P (2020) The cumulative effect of transient synchrony states on motor performance in parkinson's disease. J Neurosci 40:15711580.

Torrecillos F, Tinkhauser G, Fischer P, Green AL, Aziz TZ, Foltynie T, Limousin P, Zrinzo L, Ashkan K, Brown P, Tan H (2018) Modulation of beta bursts in the subthalamic nucleus predicts motor performance. J Neurosci 38:8905–8917. [PubMed: 30181135]

Villalba RM, Smith Y (2018) Loss and remodeling of striatal dendritic spines in parkinson's disease: From homeostasis to maladaptive plasticity? J Neural Transm (Vienna) 125:431–447. [PubMed: 28540422]

Vitrac C, Benoit-Marand MD (2017) Monoaminergic modulation of motor cortex function. Frontiers in neural circuits 11:72. [PubMed: 29062274]

Walters JR, Hu D, Itoga CA, Parr-Brownlie LC, Bergstrom DA (2007) Phase relationships support a role for coordinated activity in the indirect pathway in organizing slow oscillations in basal ganglia output after loss of dopamine. Neuroscience 144:762–776. [PubMed: 17112675]

Warlop T, Detrembleur C, Bollens B, Stoquart G, Crevecoeur F, Jeanjean A, Lejeune TM (2016) Temporal organization of stride duration variability as a marker of gait instability in parkinson's disease. J Rehabil Med 48:865–871. [PubMed: 27735982]

Whalen TC, Willard AM, Rubin JE, Gittis AH (2020) Delta oscillations are a robust biomarker of dopamine depletion severity and motor dysfunction in awake mice. Journal of neurophysiology.

Whitmer D, de Solages C, Hill B, Yu H, Henderson JM, Bronte-Stewart H (2012) High frequency deep brain stimulation attenuates subthalamic and cortical rhythms in parkinson's disease. Front Hum Neurosci 6:155. [PubMed: 22675296]

Wichmann T (2019) Changing views of the pathophysiology of parkinsonism. Mov Disord 34:1130–1143. [PubMed: 31216379]

Wichmann T, Bergman H, DeLong MR (2018) Basal ganglia, movement disorders and deep brain stimulation: Advances made through non-human primate research. J Neural Transm (Vienna) 125:419–430. [PubMed: 28601961]

Willard AM, Isett BR, Whalen TC, Mastro KJ, Ki CS, Mao X, Gittis AH (2019) State transitions in the substantia nigra reticulata predict the onset of motor deficits in models of progressive dopamine depletion in mice. eLife 8.

Williams D, Tijssen M, Van Bruggen G, Bosch A, Insola A, Di Lazzaro V, Mazzone P, Oliviero A, Quartarone A, Speelman H, Brown P (2002) Dopamine-dependent changes in the functional connectivity between basal ganglia and cerebral cortex in humans. Brain 125:1558–1569. [PubMed: 12077005]

Highlights

- Dissociation between elevated high beta LFP power in BG and PD motor symptoms is evident in 3 rat models of PD
- Increases in high beta power are preceded by loss of mid-gamma LFP oscillations in motor cortex
- Early decreases in mid-gamma cortical activity coincide with the emergence of PD motor deficits
- Phase-locking of SNpr spikes is positively correlated with gradual increases in cortical beta activity
- Changes in mid-gamma range cortical LFP activity reflect critical impact of DA loss on motor circuits

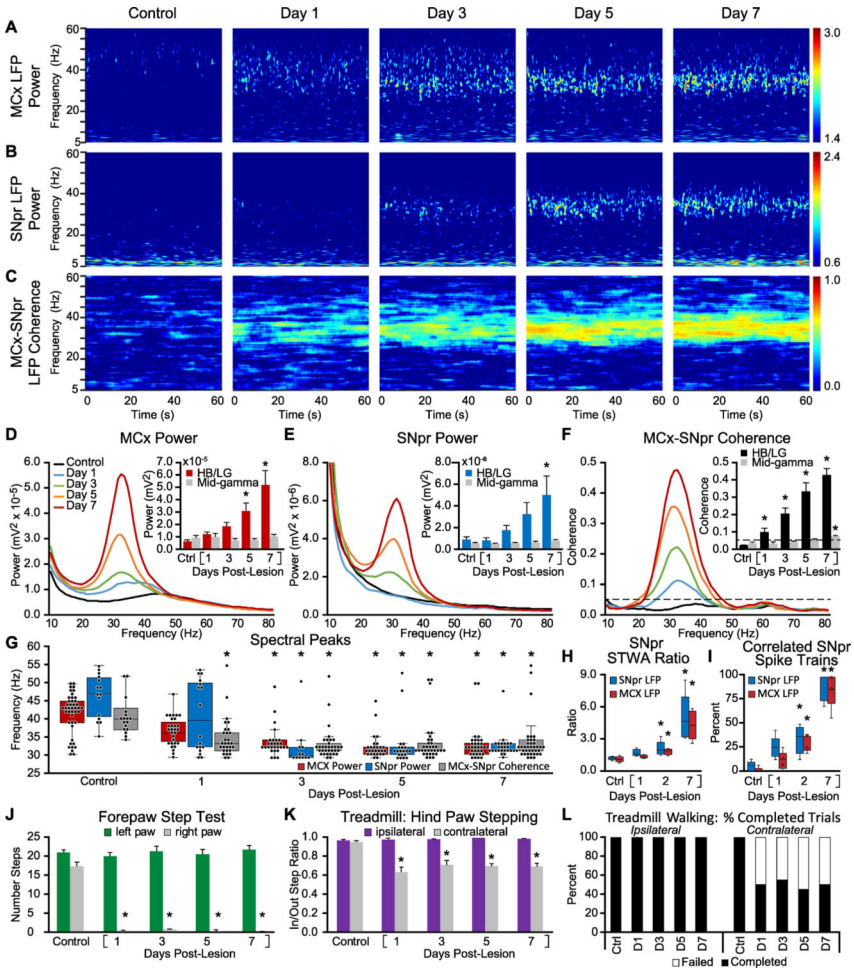

Figure 1: Alterations in MCx and SNpr high beta/low gamma LFP activity, spike-LFP relationships, LFP spectral peaks, and motor performance in the week following unilateral 6-OHDA induced dopamine cell lesion.

A-C: Representative time-frequency wavelet scalograms of spectral power in LFP recordings from MCx and SNpr, and FFT-based time-frequency MCx-SNpr coherence during treadmill walking. Recordings were obtained before injection of 6-OHDA into the median forebrain bundle (Control/Ctrl), and, starting 24 hours (Day 1) after injection, on days 1, 3, 5 and 7. Power is plotted on a logarithmic scale and coherence spectrograms are plotted on a linear scale with greater values represented by red. **D-F:** Averaged MCx and SNpr LFP power spectra and MCx-SNpr coherence spectra with bar graphs (inset) depicting mean total LFP power around dominant peaks (peak +/− 3 Hz) in the high beta/low gamma (HB/LG) 29–40 Hz frequency range in the MCx (**D**, red bars), SNpr (**E**, blue bars) and MCx-SNpr coherence (**F**, black bars), and in the mid-gamma 40–55 Hz range (**D-F** grey bars). Bar graphs show linear increases in MCx and SNpr HB/LG LFP power ($R^2 = 0.94$) and MCx-SNpr coherence ($R^2 = 0.99$) over days 1, 3, 5 and 7 following the 6-OHDA injection. Data are reported as mean ± SEM. * $p < 0.05$, relative to control (Ctrl). **G:** Distribution of the frequencies of dominant spectral peaks in MCx and SNpr LFP power and MCx-SNpr coherence spectra in recordings from before lesion (Control) and on days 1, 3, 5 and 7 after unilateral dopamine cell lesion during treadmill walking. Box plots

depict 25th to 75th percentile values and black dots show individual peak frequencies. * $p < 0.05$, relative to control, n = 9 rats, max 8 peaks per rat, see methods). **H-I:** Spike-LFP phase-locking of spikes from SNpr multiunit spike-trains with SNpr and MCx LFP activity in the HB/LG range from control rats and on 1, 2, and 7 days post-lesion. Box plots **(H)** show ratios of unshuffled:shuffled peak-to-trough amplitude in STWAs (see Methods) and **(I)** the proportion of multi-unit SNpr spike trains with spikes significantly correlated to SNpr LFPs (blue bars) and MCx LFP (red bars). * $p < 0.05$, relative to control, n = 64 multiunit spike trains, 2 epochs/train, 4–8 trains per rat, 5 rats). **J-L:** Motor function in control rats and following unilateral DA cell lesion. **J:** Bar graph shows the number of steps made by the right paw and the left paw in the forelimb step test in control and over days 1–7 post-lesion. **K:** Bar graph displays inner:outer hind limb step count ratios during ipsilateral (purple bars) and contralateral (gray bars) walking in a circular treadmill. **L:** Bar graph indicates the % completed trials (black bars) vs incidences of failure (white bars) to initiate and maintain steady treadmill walking for at least 30 seconds when oriented in the direction contralateral to the lesion. * $p < 0.05$, relative to control.

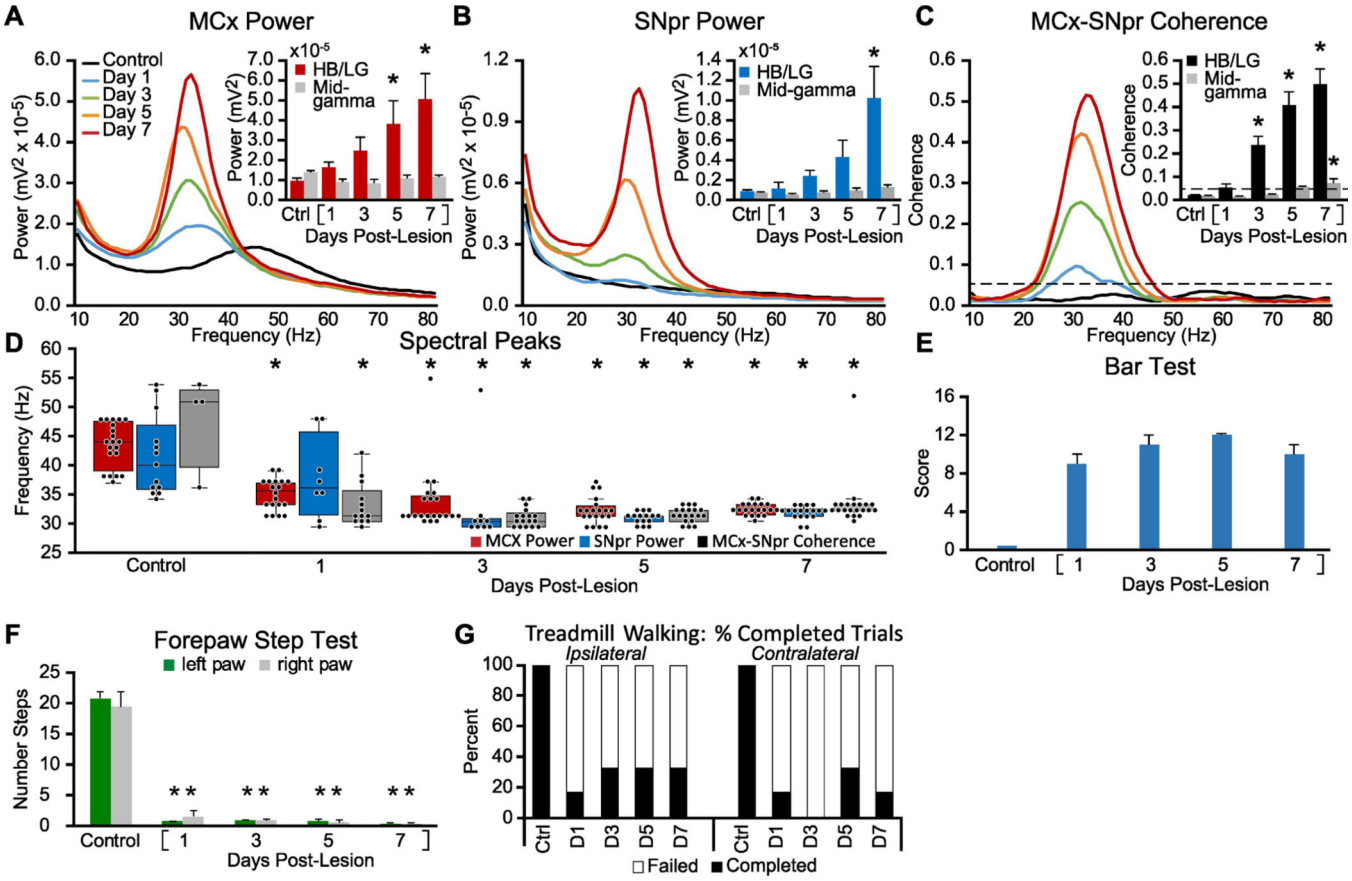

Figure 2: Alterations in MCx and SNpr high beta/low gamma LFP activity, LFP spectral peaks, and motor performance in the week following bilateral 6-OHDA induced dopamine cell lesion.

Recordings were obtained before (Control/Ctrl) and after bilateral DA-cell lesion on days 1, 3, 5, and 7 during epochs of intermittent walking in an open cylinder rotating at a reduced speed (5 RPM vs. 9 RPM, see methods). **A-C:** Averaged MCx and SNpr LFP power spectra and MCx-SNpr coherence spectra with bar graphs (inset) depicting mean total LFP power around dominant peaks in the HB/LG frequency range in the MCx (**D**, red bars), SNpr (**E**, blue bars) and MCx-SNpr coherence (**F**, black bars), and in the mid-gamma range (**D-F** grey bars). Bar graphs show linear increases in MCx ($R^2 = 0.98$), and SNpr ($R^2 = 0.97$) HB/LG oscillatory activity and MCx-SNpr coherence ($R^2 = 0.96$) following the 6-OHDA injection relative to control (Ctrl). * $p < 0.05$, relative to control. **D:** Dominant spectral peaks in MCx and SNpr LFP power and MCx-SNpr coherence spectra in recordings from before and after bilateral 6-OHDAmediated dopamine cell lesion during treadmill walking. Box plots depict 25^{th} to 75^{th} percentile values and black dots show individual peak frequencies in the 29 – 55 Hz range. * $p < 0.05$, relative to control. **E-G:** Motor function in control rats and following bilateral DA cell lesion. **E:** Bar graph shows stable catalepsy starting from day 1 post-lesion (2 rats). **F:** Bar graph shows number of steps made by the right and left paws in the forelimb step test during control and post-lesion days compared to control. **G:** Bar graph indicates the % completed trials (black bars) vs incidences of failure (white bars) to initiate and maintain steady treadmill walking for at least 30 seconds when oriented in the direction contralateral to the lesion. * $p < 0.05$, relative to control, n = 3 rats.

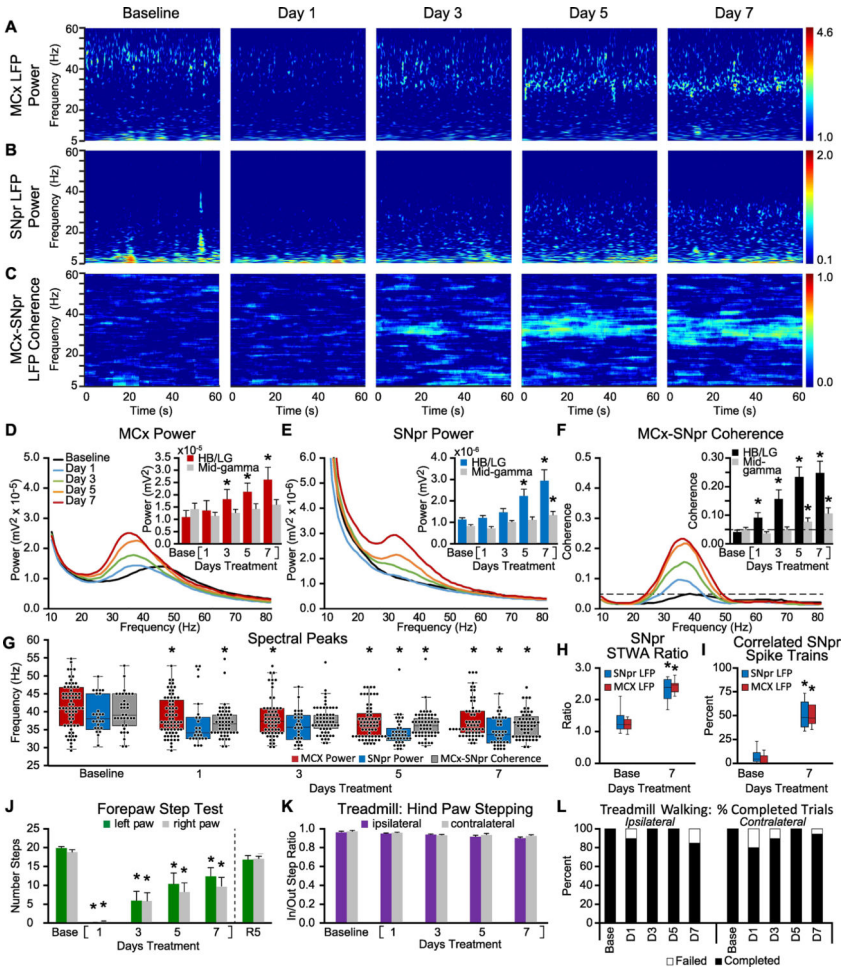

Figure 3: Alterations in MCx and SNpr HB/LG LFP activity, spike-LFP relationships and motor performance over one week of chronic treatment with dopamine receptor D1 and D2 antagonists.

A-C: Representative time-frequency wavelet scalograms of spectral power in LFP recordings from MCx and SNpr, and FFT-based time-frequency MCx-SNpr coherence during treadmill walking. Recordings were obtained prior to (Baseline/Base) and over one week of chronic, twice-daily treatment with D1+D2 antagonists on days 1, 3, 5 and 7 at 10 AM and 5 PM, prior to the first treatment of D1+D2 antagonists. Power is plotted on a logarithmic scale and coherence spectrograms are plotted on a linear scale with greater values represented by red. **D-F:** Averaged MCx and SNpr LFP power spectra and MCx-SNpr coherence spectra with bar graphs (inset) depicting mean total LFP power around dominant peaks in the HB/LG frequency range in the MCx (**D**, red bars), SNpr (**E**, blue bars) and MCx-SNpr coherence (**F**, black bars), and in the mid-gamma range (**D-F** grey bars). Bar graphs depict linear increases in HB/LG LFP power over days 1, 3, 5 and 7 of treatment in MCx ($R^2 = 0.90$) and SNpr ($R^2 = 0.94$) and HB/LG MCx-SNpr coherence ($R^2 = 0.95$). * $p < 0.05$, relative to baseline (Base). **G:** Dominant peaks in MCx and SNpr LFP power and coherence spectra. Box plots show median and 25th to 75th percentile values as well as individual peak frequencies (black dots) for dominant peaks in MCx and SNpr power and MCx-SNpr coherence at baseline and on days 1, 3, 5 and 7 following chronic

treatment with D1+D2 antagonists. * $p < 0.05$, relative to baseline, max n = 120 peaks, 15 rat hemispheres, see methods. **H-I:** Spike-LFP phase-locking of spikes from SNpr multiunit spike-trains with HB/LG SNpr and MCx LFP activity at baseline and at day 7 of chronic DA antagonist treatment. **H:** Box plots show unshuffled:shuffled peak-to-trough STWA ratios of SNpr spike trains correlated to SNpr LFPs or to MCx LFPs. **I:** Box plots show proportion of multiunit SNpr spike trains with spikes significantly correlated to SNpr and MCx LFPs. * $p < 0.05$, relative to baseline, n = 144 multiunit spike trains, 2 epochs/train, 4–8 trains per rat, 10 hemispheres). **JL:** Motor function at baseline and following chronic treatment with D1+D2 antagonists. **J:** Bar graphs show the number of steps made by the right paw and left paws in forelimb step test at baseline and at days 1, 3, 5 and 7 and after a 5 day recovery without antagonist treatment (R5). **K:** Bar graph displays inner:outer hind limb step count ratios during ipsilateral (purple bars) and contralateral (gray bars) walking on the circular treadmill at baseline and over days 1, 3, 5 and 7. **L:** Bar graph indicates the % completed trials (black bars) vs incidences of failure (white bars) to initiate and maintain steady treadmill walking for at least 30 seconds when oriented in the direction contralateral to the lesion. * $p < 0.05$, relative to baseline

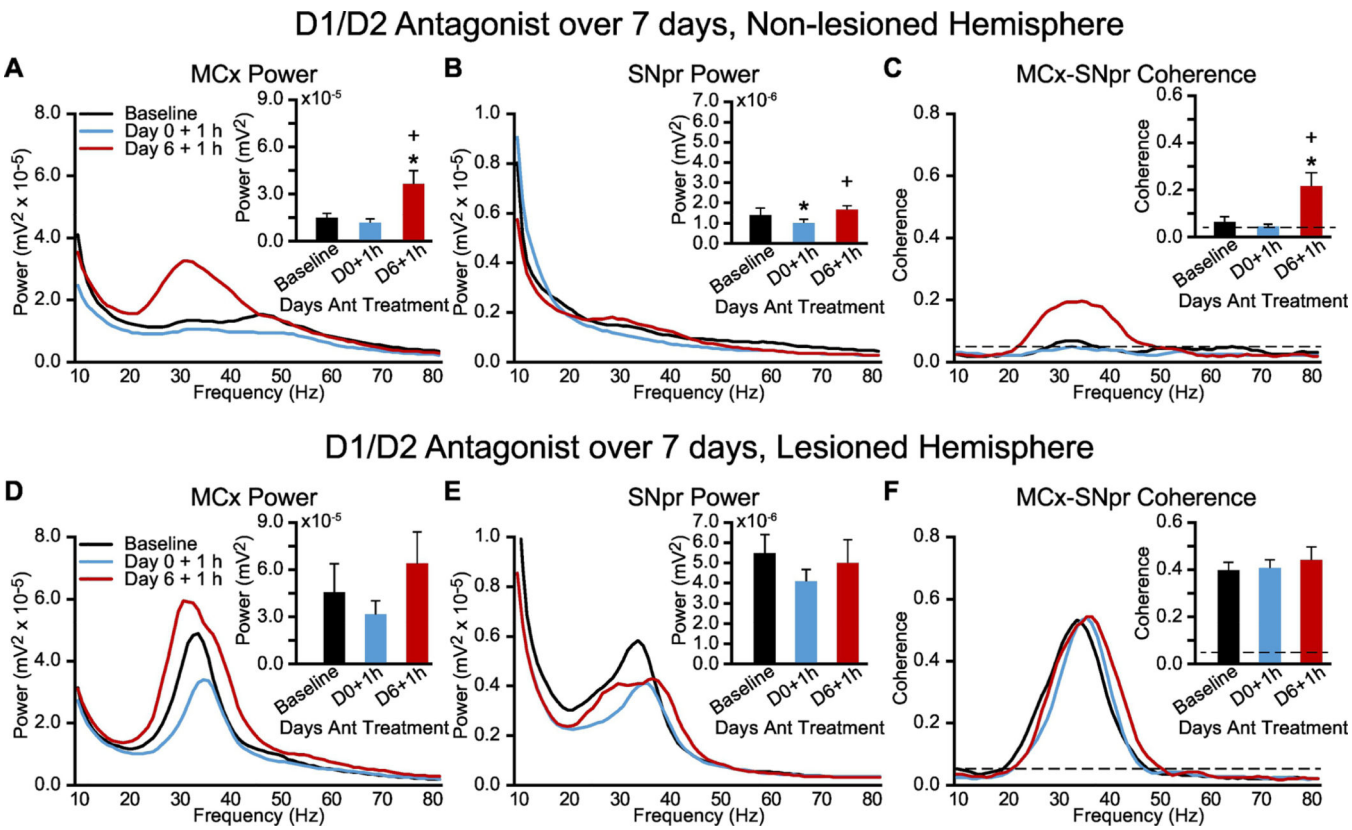

Figure 4: Alterations in MCx and SNpr HB/LG LFP activity in lesioned and non-lesioned hemispheres of unilaterally DA-cell-lesioned rats over one week of chronic treatment with dopamine receptor D1 and D2 antagonists.

Recordings were obtained during treadmill walking before commencement of chronic drug treatment (Baseline) and 1 hour after drug administration on the first (Day 0 + 1 h) and seventh (Day 6 + 1 h) days of chronic antagonist treatment during periods of catalepsy (with manually induced movement, see methods). **A-C, Non-lesioned hemisphere:** Averaged MCx LFP power spectra (**A**) and SNpr LFP power spectra (**B**) and MCx-SNpr coherence spectra (**C**) with bar graphs (inset) depicting mean total LFP power or coherence around dominant peaks in the HB/LG frequency range at Baseline (black bars), on the first day of treatment (Day 0 + 1 h, blue bars) and on the seventh day of treatment (Day 6 + 1 h, red bars). **D-F, Lesioned hemisphere:** Averaged MCx LFP power spectra (**D**) and SNpr LFP power spectra (**E**) and MCx-SNpr coherence spectra (**F**) with bar graphs (inset) depicting mean total LFP power or coherence around dominant peaks in the HB/LG frequency range at Baseline (black bars), on the first day of treatment (Day 0 + 1 h, blue bars) and on the seventh day of treatment (Day 6 + 1 h, red bars). * $p < 0.05$, relative to baseline.

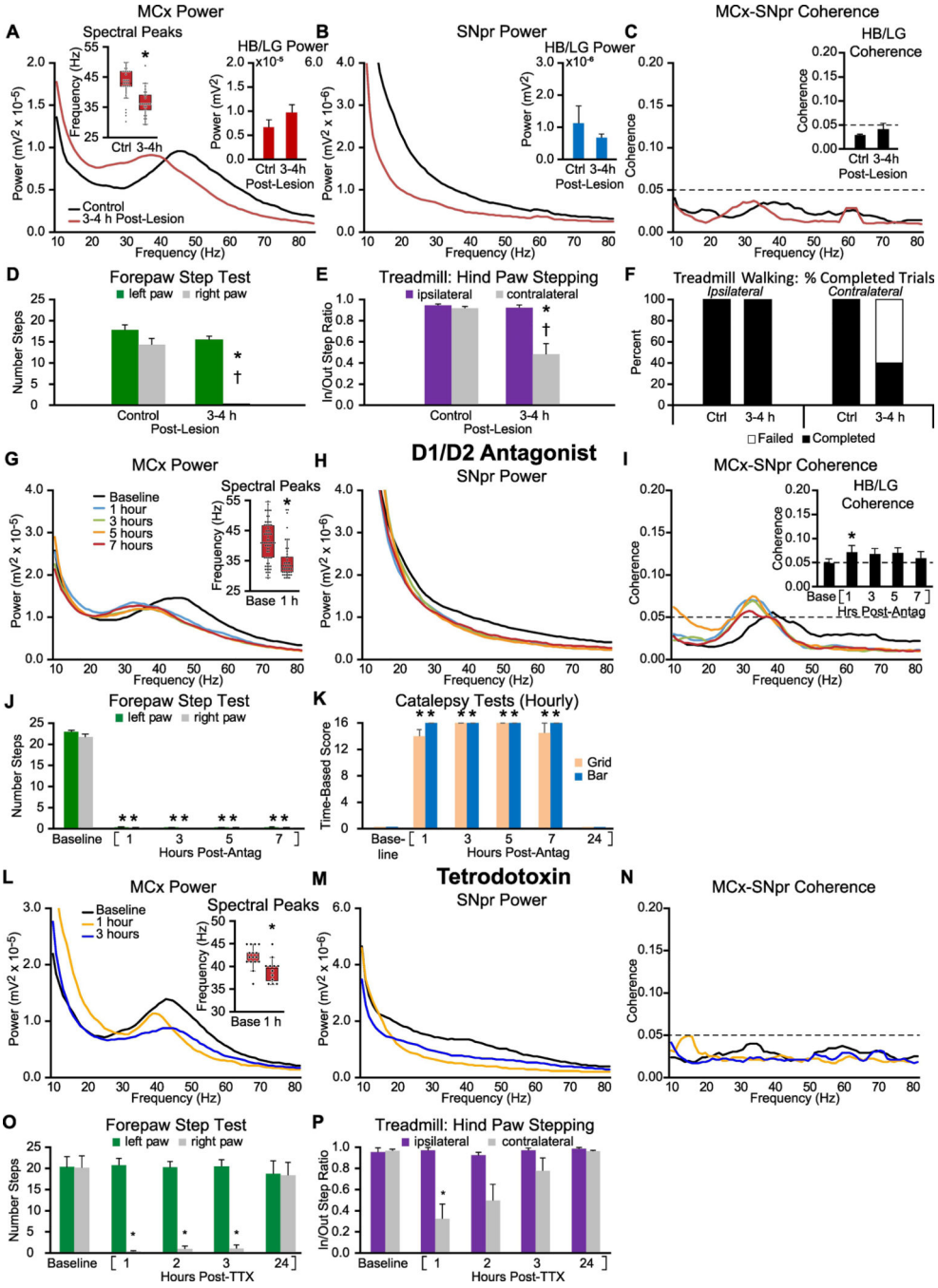

Figure 5: Early alterations in MCx and SNpr high beta/low gamma LFP activity and motor performance in the hours following either unilateral 6-OHDA induced dopamine cell lesion (A-F), single administration of D1+D2 antagonists (G-K), or MFB infusion of TTX (L-P)

A-C: Averaged MCx and SNpr LFP power spectra and MCx-SNpr coherence spectra before (Ctrl) and 3–4 hours after unilateral DA-cell lesion during epochs of treadmill walking. Bar graphs (inset) depict mean total LFP power around dominant peaks in the HB/LG frequency range in the MCx (**A**, red bars), SNpr (**B**, blue bars) and MCx-SNpr coherence (**C**, black bars). Box plot inset in **A** depicts median peak frequencies of dominant peaks before and after lesion. * $p < 0.05$, relative to control (Ctrl). **D-F:** Motor function in control rats and

3–4 h following unilateral DA cell lesion. **D:** Bar graph shows the number of steps made by the right paw and the left paw in the forelimb step test in control and post-lesion. **E:** Bar graph displays inner:outer hind limb step count ratios during ipsilateral (purple bars) and contralateral (gray bars) walking in a circular treadmill. **F:** Bar graph indicates the % completed trials (black bars) vs incidences of failure (white bars) to initiate and maintain steady treadmill walking for at least 30 seconds when oriented in the direction contralateral to the lesion. * $p < 0.05$, relative to control, † $p < 0.05$, contralateral vs. ipsilateral **G-I:** Averaged LFP power and MCx-SNpr coherence spectra at baseline (Base) and over 7 hours following treatment with D1+D2 antagonists. Box plot inset in **G** depicts median peak frequencies of dominant peaks before and 1 hour following treatment. Bar graph inset in **I** depicts mean MCx-SNpr coherence (black bars). **J-K:** Motor function at baseline and over 7 hours following D1+D2 antagonist treatment. **J:** Bar graphs show the number of steps made by the right paw and left paws in forelimb step test at baseline and at hours 1, 3, 5 and 7 following the first dose. **K:** Bar graph depicts assessments of catalepsy as measured by grid (beige) and bar (blue) tests. * $p < 0.05$, relative to baseline. **L-N:** Averaged LFP power and MCx-SNpr coherence spectra during treadmill walking at baseline and over 24 hours following infusion of TTX. Box plot inset in **L** depicts median peak frequencies of dominant peaks before and 1 hour following infusion. * $p < 0.05$, relative to baseline. **O-P:** Motor function before and following infusion of TTX. **O:** Bar graphs show the number of steps made by the right paw and left paws in forelimb step test at baseline and at hours 1, 2, 3, and 24 following treatment. **P:** Bar graph displays inner:outer hind limb step count ratios during ipsilateral (purple bars) and contralateral (gray bars) walking on the circular treadmill at baseline and over hours 1, 2, 3, and 24. * $p < 0.05$, relative to baseline.

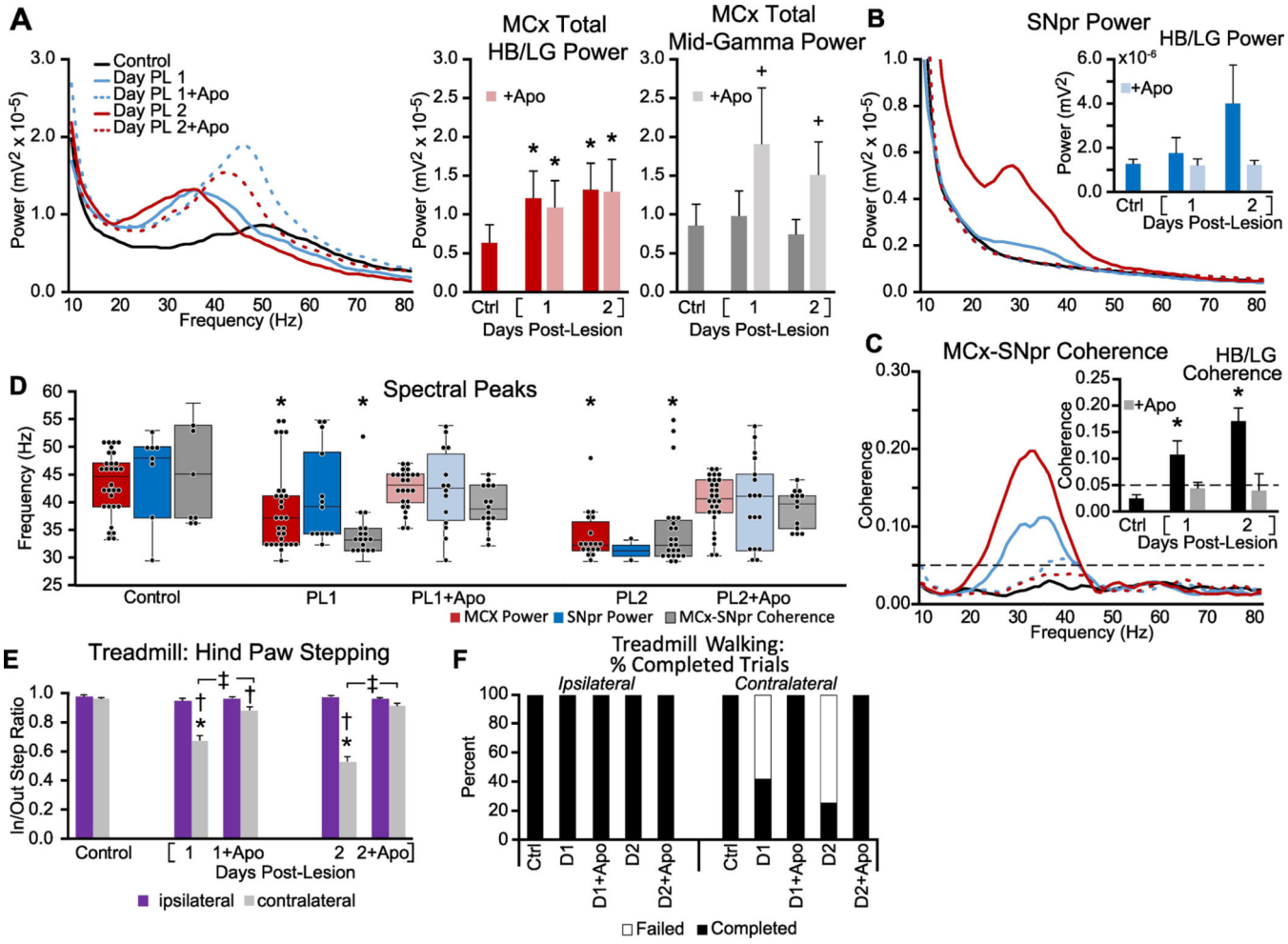

Figure 6: Acute effects of apomorphine-induced stimulation of dopamine receptors on MCx and SNpr high beta/low gamma LFP activity and motor performance on days 1 and 2 after unilateral 6-OHDA-induced DA cell loss.

A-C: Averaged MCx and SNpr LFP power spectra and MCx-SNpr coherence spectra with bar graphs (inset in **B, C**) depicting mean total LFP power around dominant peaks in the HB/LG frequency range in the MCx (**A**, red bars), SNpr (**B**, blue bars), and MCx-SNpr coherence (**C**, black bars) during treadmill walking in control (Ctrl), at 24 h and 48 h after DA cell lesion (Day PL 1 and Day PL 2, respectively) and following systemic injection of apomorphine (Day PL 1 + Apo and Day PL 2 + Apo, represented by lighter bars). * $p < 0.05$, relative to control, + $p < 0.05$, relative to pre-apomorphine. **D**: Distribution of the frequencies of dominant spectral peaks in MCx and SNpr LFP power and MCx-SNpr coherence spectra in recordings during treadmill walking in control, at Day PL 1 and Day PL 2, and following systemic injection of apomorphine. Box plots depict 25th to 75th percentile values and black dots show individual peak frequencies. *$p < 0.05$, relative to control, n = 6 rats, max 8 peaks per rat, see methods). **E-F**: Motor function in control rats and following DA-cell lesion with and without apomorphine. **E**: Bar graph displays inner:outer hind limb step count ratios during ipsilateral (purple bars) and contralateral (gray bars) walking in a circular treadmill. **F**: Bar graph indicates the % completed trials (black

bars) vs incidences of failure (white bars) to initiate and maintain steady treadmill walking for at least 30 seconds when oriented in the direction contralateral to the lesion. * $p < 0.05$, relative to control, † $p < 0.05$, contralateral vs. 1343versive, ‡ $p < 0.05$, Day 1 + Apo vs. Day 2 + Apo